Euro. Jnl of Applied Mathematics (2004), *vol.* 15, *pp.* 713–754. © 2004 Cambridge University Press
doi:10.1017/S0956792504005753 Printed in the United Kingdom

Moving-boundary and fixed-domain problems for a sixth-order thin-film equation

J. C. FLITTON and J. R. KING

Theoretical Mechanics Section, School of Mathematical Sciences, University of Nottingham, NG7 2RD, UK
email: john.king@nottingham.ac.uk

(*Received 25 September 2003; revised 26 July 2004*)

We examine a number of initial boundary value problems for a paradigm sixth-order degenerate parabolic equation of the form $h_t = (h^n h_{xxxxx})_x$ which arises when considering the motion of a thin film of viscous fluid driven by an overlying elastic plate. Analytical and numerical methods are exploited to characterise the solutions, which turn out to be rather sensitive to the value of n.

1 Introduction

This paper is concerned with the sixth-order nonlinear diffusion equation

$$\frac{\partial h}{\partial t} = \frac{\partial}{\partial x}\left(h^n \frac{\partial^5 h}{\partial x^5}\right), \tag{1.1}$$

where $h \geqslant 0$ will be treated as the thickness of a fluid film beneath an elastic plate and $p = \partial^4 h/\partial x^4$ as the pressure within the film [14]. For future reference we note that we can in the usual way assign physical meaning to some of the other derivatives of h, specifically

$$m = -\frac{\partial^2 h}{\partial x^2}, \quad \Sigma = \frac{\partial^3 h}{\partial x^3} \tag{1.2}$$

where m is the bending moment on the overlying plate and Σ the shearing force [19]; all such expressions here are dimensionless ones. An equation of this type can be used to model the motion of a thin film of viscous fluid overlain by an elastic plate [15]; see also Hobart *et al.* [11] and Huang & Suo [13] for possible applications of such modelling approaches to the wrinkling upon annealing of SiGe films bonded to Si substrates. Other plausible applications of (1.1), and suitable generalisations thereof, include as a simple model for the influence of a crust on a solidifying melt or for a microfluidic pump (see Koch *et al.* [18], for instance).

Equation (1.1) is the third of a hierarchy arising from the generalised Reynolds equation

$$\frac{\partial h}{\partial t} = \frac{\partial}{\partial x}\left(h^n \frac{\partial p}{\partial x}\right), \tag{1.3}$$

under different driving forces. For gravity driven flows, we have $p = h$, giving the very

https://doi.org/10.1017/S0956792504005753 Published online by Cambridge University Press

widely studied porous-medium equation (see, for example, Aronson [1]). For surface tension driven flows we have $p = -\partial^2 h/\partial x^2$, leading to the "thin-film" equation, which has been the subject of a great deal of recent study (see Hulshof [12], for instance). The sixth-order case (1.1) has been much less extensively investigated (though see Smyth & Hill [21], Bernis & Friedman [3], Smith *et al.* [20], Evans *et al.* [10] and Barrett *et al.* [2] for examples of existing studies, the first two being analytical and the others primarily numerical) and we endeavour here to give a reasonably comprehensive classification of those properties which relate inextricably to its degeneracy at $h = 0$; we do this by focusing on three specific initial boundary value problems which we describe below. For much of the range of n its behaviour follows very closely that of the corresponding fourth-order case (see Bowen & King [6, 17], in particular), but, as we shall see, there is a range of n in which entirely new phenomena occur.

Our focus here is not primarily on physical applications, but we should record that for Newtonian viscous fluids which do not slip along the substrate $n = 3$ pertains in (1.3), while the Navier-slip dominated case has $n = 2$. The study of other values of n can be motivated by, *inter alia*, applications to power-law fluids spreading over horizontal substrates (the precise model differs somewhat, but the structure of the solutions is very closely related – see § 7), with $n > 3$ corresponding to shear-thickening fluids and $n < 3$ to shear-thinning ones (cf. Bowen *et al.* [7] for further discussion on such matters). Moreover, (1.3) is itself relevant to power-law fluids spreading across a slightly inclined substrate (see King [16]), now with $n < 3$ corresponding to shear-thickening fluids and $n > 3$ to shear-thinning ones. Finally, $n = 1$ arises for thin-film flows in a Hele–Shaw cell [8, 9]. Here we regard (1.1) as a prototype sixth-order parabolic equation and investigate the variety of properties that it can exhibit. An alternative hierarchy to the one based on (1.3) has flow by (mean) curvature as its second-order member and flow by the Laplacian of curvature as its fourth-order one; the analogous sixth-order case here would of course involve the surface biharmonic operator in place of the Laplacian.

We now outline the three specific initial boundary value problems with which we shall concern ourselves. The first is the Cauchy problem, with

$$\text{at} \quad t = 0 \quad h = h_i(x) \tag{1.4}$$

where $h_i(x) = 0$ for $|x| > a$ and $h_i(x) > 0$ for $|x| < a$ and $h(x,t) = 0$ for $|x| > s(t)$, say (where $s(0) = a$; for brevity we restrict ourselves to initial data (and hence solutions) symmetric about $x = 0$), with

$$\int_{-s(t)}^{s(t)} h(x,t)dx = \int_{-a}^{a} h_i(x)dx \equiv M \tag{1.5}$$

for some constant M. We have the moving boundary conditions

$$\text{at} \quad x = s(t) \quad h = 0, \quad h^n \frac{\partial^5 h}{\partial x^5} = 0, \tag{1.6}$$

the first defining the moving boundary and the second required for conservation of mass; with a sixth-order problem with an *a priori* unknown moving boundary $s(t)$, this leaves us two conditions short, so the difficulties present in the fourth-order case described in

https://doi.org/10.1017/S0956792504005753 Published online by Cambridge University Press

King & Bowen [17] are compounded. Secondly, we consider the fixed domain problem in which (1.4) holds with

$$\text{at} \quad x = a \quad h = 0 \tag{1.7}$$

again leaving us two conditions short (cf. Bowen & King [6] for the fourth-order case). Finally, we investigate the "dipole" problem (cf. Bernis *et al.* [4]), which can be regarded as a combination of the above two in which (1.6) still holds (on the right-hand interface $x = s(t)$) and at the left-hand end we have the fixed domain condition

$$\text{at} \quad x = 0 \quad h = 0. \tag{1.8}$$

We study these problems by a combination of asymptotic and numerical methods, starting by investigating the relevant local balances to classify the possible non-negative solution branches and then investigating in detail the smoothest such solutions; in the Cauchy and dipole cases the numerics are based on introducing a thin prewetting layer (of thickness ϵ) to relieve the contact-line singularity as $x = s(t)$ and to avoid the numerical difficulty of tracking an unknown moving interface. For brevity, we largely restrict ourselves to the case $n > 0$, though many of the conclusions in fact follow through to $n \leqslant 0$.

2 Local behaviour of solutions

2.1 Preliminaries

Here we investigate the possible local behaviour of solutions close to a zero of h (i.e. depending on which of the three problems we are concerned with, close to $x = 0$, $x = a$ or $x = s(t)$), exploiting in doing so some simple explicit solutions to (1.1). We sub-divide the classification into three, firstly considering fixed fronts (at $x = a$) with zero flux of fluid through the front, the flux into the fluid domain at a right-hand interface being given by

$$J(t) = h^n \frac{\partial^5 h}{\partial x^5}. \tag{2.1}$$

Secondly, we treat fixed fronts with $J \neq 0$ and, finally, we examine moving fronts ($\dot{s} \neq 0$) with $J = 0$.

All solutions in this section take the form

$$h \sim A(t)(s(t) - x)^p \quad \text{as} \quad x \to s^-; \tag{2.2}$$

for fixed front cases we set $s(t) = a$ (an obvious change of sign is needed in addressing the limit $x \to 0^+$, say). The resulting classification is summarised in Figure 1.

The following subsections list the possible behaviours and indicate their possible relevance in terms of numbers of boundary conditions; the classification will be crucial to our subsequent analysis. We omit discussion of the borderline cases where logarithmic terms also appear. Throughout this section the functions $A_i(t)$ are arbitrary in the local expansion, while the $B(t)$ are known functions of the A_i and hence do not represent additional degrees of freedom.

https://doi.org/10.1017/S0956792504005753 Published online by Cambridge University Press

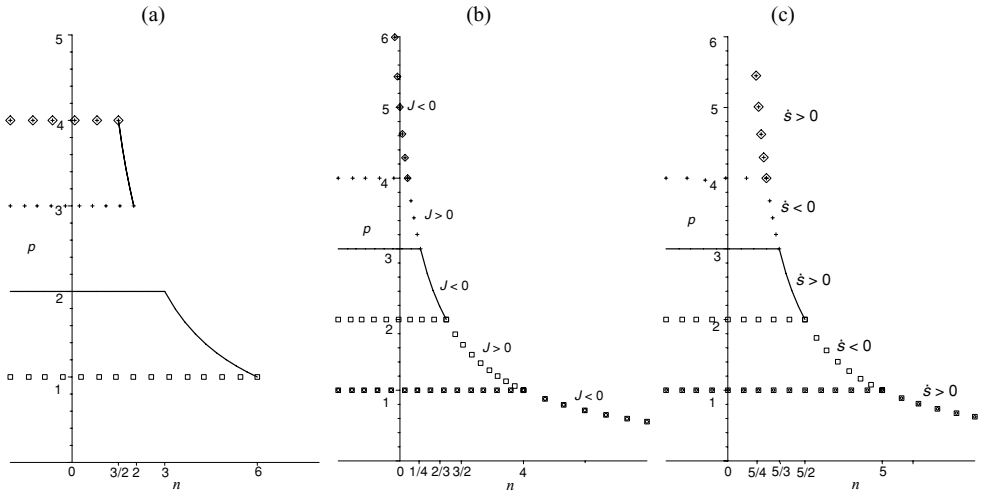


FIGURE 1. Solution branches, classified according to whether doubly underspecified (○ inside □), singly underspecified (□), correctly specified (——), singly overspecified (+), doubly overspecified (+ inside ⋄). (a) Zero-flux fixed-front cases; the curve on the right has $p = 6/n$. (b) Finite-flux fixed-front cases; the curve has $p = 5/(n+1)$. (c) Moving-front zero-flux cases; the curve has $p = 5/n$. There are no constraints on the sign of J (in (b)) and $\dot{s}$ (in (c)) on the horizontal branches.

2.2 Fixed front, zero flux, $s = a$, $J = 0$

Firstly, we have separable solutions which are correctly specified (i.e. have three degrees of freedom in the local expansion) for $3/2 < n < 2$ and $3 < n < 6$ on which $p = 6/n$ in (2.2) and

$$A(t) = \left(\frac{n^5}{72(n+6)(2n-3)(n-2)(n-3)(6-n)t} \right)^{1/n}; \tag{2.3}$$

this provides an exact solution to (1.1) (cf. Smyth & Hill [21]). For $3/2 < n < 3$ the expansion

$$h(x) \sim A_0(t)(a-x)^2 + A_1(t)(a-x)^3 + A_2(t)(a-x)^4 + B(t)(a-x)^{8-2n} \quad \text{as} \quad x \to a^-, \tag{2.4}$$

where

$$B(t) = \frac{A_0^{-n}\dot{A}_0}{3(2n-4)(2n-5)(2n-6)(2n-7)(2n-8)}, \tag{2.5}$$

also contains three degrees of freedom, namely A_0, A_1 and A_2. The B term should clearly appear earlier in the sequence if $n > 2$. These two solution branches are represented by the solid curves in Figure 1(a).

Another possible branch is a locally linear, taking the form

$$h(x) \sim A_0(t)(a-x) + A_1(t)(a-x)^2 + A_2(t)(a-x)^3 + A_3(t)(a-x)^4 + B(t)(a-x)^{7-n} \quad \text{as} \quad x \to a^-, \tag{2.6}$$

https://doi.org/10.1017/S0956792504005753 Published online by Cambridge University Press

where

$$B(t) = \frac{A_0^{-n}\dot{A}_0}{2(n-3)(n-4)(n-5)(n-6)(n-7)}, \tag{2.7}$$

and thus being applicable (self-consistent) for $n < 6$; this branch in singly underspecified, containing the four degrees of freedom A_0, A_1, A_2 and A_3. A singly overspecified (two degrees of freedom, A_0 and A_1) branch is given by

$$h(x) \sim A_0(t)(a-x)^3 + A_1(t)(a-x)^4 + B(t)(a-x)^{8-2n} \quad \text{as} \quad x \to a^- \tag{2.8}$$

where

$$B(t) = \frac{A_0^{-n}\dot{A}_0}{4(3n-5)(3n-6)(3n-7)(3n-8)(3n-9)}, \tag{2.9}$$

which is admissible for $n < 2$, while a locally quartic doubly overspecified branch (A_0 being the only degree of freedom) is

$$h(x) \sim A_0(t)(a-x)^4 + B(t)(a-x)^{8-2n} \quad \text{as} \quad x \to a^- \tag{2.10}$$

where

$$B(t) = -\frac{A_0^{-n}\dot{A}_0}{5(4n-6)(4n-7)(4n-8)(4n-9)(4n-10)}. \tag{2.11}$$

Each of these branches is illustrated in Figure 1(a), with the transfer between branches naturally occurring where $6/n$ passes through the integers $p = 1, 2, 3, 4$, which correspond to steady-state solutions of (1.1). It is striking that no branches have been identified in $n > 6$, an issue to which we shall need to return and examine in detail.

2.3 Fixed front, non-zero flux, $s = a$, $J \neq 0$.

The $5/(n+1)$ curve shown in Figure 1(b) corresponds to the local solution

$$h(x) \sim A_0(t)(a-x)^{5/(n+1)} \quad \text{as} \quad x \to a^-, \tag{2.12}$$

where

$$A_0(t) = \left(-\frac{J(t)(n+1)^5}{5(4n-1)(3n-2)(2n-3)(n-4)}\right)^{1/(n+1)}. \tag{2.13}$$

The sign of J is significant as the solution holds with positive J, a mass flux into the domain, being required for $1/4 < n < 2/3$ and $3/2 < n < 4$ and with negative J, "drainage" of fluid, being necessary for $n < 1/4$, $2/3 < n < 3/2$ and $n > 4$. For J constant this is an exact (steady-state) solution to (1.1), but for arbitrary J, subject to these constraints on sign, it provides a possible local behaviour for $n > -1$. The degrees of freedom for this branch are given by $J(t)$ together with the eigenmodes obtained by linearising (2.1) about (2.12)-(2.13) and identifying the solutions $(a-x)^{5/(n+1)+Q}$ of the resulting Euler equation which have $\mathrm{Re}(Q) > 0$. The results are summarised in Figure 1(b) with, for example, two eigenmodes having $\mathrm{Re}(Q) > 0$ for $2/3 < n < 3/2$, giving a correctly specified branch. The other correctly specified solution branch shown in Figure 1(b)

https://doi.org/10.1017/S0956792504005753 Published online by Cambridge University Press

has

$$h(x) \sim A_0(t)(a-x)^3 + A_1(t)(a-x)^4 + A_2(t)(a-x)^{5-3n} \quad \text{as} \quad x \to a^-, \tag{2.14}$$

requiring $n < 2/3$, where

$$A_2(t) = \frac{A_0^{-n} J(t)}{(3n-1)(3n-2)(3n-3)(3n-4)(3n-5)}. \tag{2.15}$$

Here J is arbitrary and hence the three degrees of freedom are A_0, A_1 and $J(t)$. The other solution branches correspond to the following local expansions. The doubly underspecified finite contact-angle solution in $n < 4$ has (for $n \neq 1$, 2 or 3, to avoid logarithmic terms; we omit such qualifications elsewhere here)

$$h(x) \sim A_0(t)(a-x) + A_1(t)(a-x)^2 + A_2(t)(a-x)^3 + A_3(t)(a-x)^4 + A_4(t)(a-x)^{5-n} \quad \text{as} \quad x \to a^-, \tag{2.16}$$

where

$$A_4(t) = \frac{A_0^{-n} J(t)}{(n-1)(n-2)(n-3)(n-4)(n-5)}, \tag{2.17}$$

the five degrees of freedom being A_0, A_1, A_2, A_3 and J. For $n > 1$ the A_4 term is larger than some of the preceding ones. A locally parabolic, singly underspecified solution of the form

$$h(x) \sim A_0(t)(a-x)^2 + A_1(t)(a-x)^3 + A_2(t)(a-x)^4 + A_3(t)(a-x)^{5-2n} \quad \text{as} \quad x \to a^-, \tag{2.18}$$

where

$$A_3(t) = \frac{A_0^{-n} J(t)}{(2n-1)(2n-2)(2n-3)(2n-4)(2n-5)}, \tag{2.19}$$

is possible for $n < 3/2$. Here the four degrees of freedom are A_0, A_1, A_2 and J. In this case the final term should be moved up the expansion if $n > 1/2$. Finally, the expansion

$$h(x) \sim A_0(t)(a-x)^4 + A_1(t)(a-x)^{5-4n} \quad \text{as} \quad x \to a^-, \tag{2.20}$$

where

$$A_1(t) = \frac{A_0^{-n} J(t)}{(4n-1)(4n-2)(4n-3)(4n-4)(4n-5)}, \tag{2.21}$$

is admissible for $n < 1/4$ and has two degrees of freedom, A_0 and J.

2.4 Moving fronts, zero flux, $\dot{s} \neq 0$, $J = 0$.

The final forms of solution we investigate can apply at a moving boundary at which mass is conserved. In this regime we find the behaviours by considering solutions to the balance

$$\dot{s} \sim -h^{n-1} \frac{\partial^5 h}{\partial x^5} \quad \text{as} \quad x \to s^-(t) \tag{2.22}$$

which arises locally because the time derivative is dominated by its convective part. We note that (2.22) corresponds to (2.1) with n replaced by $n-1$ and J by $-\dot{s}$, so the

https://doi.org/10.1017/S0956792504005753 Published online by Cambridge University Press

conclusions follow directly from those of the previous subsection. The solution

$$h(x) \sim A_0(t)(s-x)^{5/n} \quad \text{as} \quad x \to s^-, \tag{2.23}$$

where

$$A_0(t) = \left(-\frac{n^5 \dot{s}}{5(4n-5)(3n-5)(2n-5)(n-5)} \right)^{1/n}, \tag{2.24}$$

exists for a spreading front, $\dot{s} > 0$, for $n < 5/4$, $5/3 < n < 5/2$ and $n > 5$, while retracting front ($\dot{s} < 0$) solutions of this type can occur for $5/4 < n < 5/3$ and $5/2 < n < 5$. The number of degrees of freedom associated with such a solution, in addition to $s(t)$, can be determined by linearising (2.22) about (2.23)–(2.24). The correctly-specified section of this curve in Figure 1(c) occurs in $5/3 < n < 5/2$, in which it represents an advancing front ($\dot{s} > 0$). Expressions (2.23)–(2.24) provide an exact (travelling-wave) solution to (1.1) when $\dot{s}$ is constant. The other correctly specified branch in Figure 1(c) has the form

$$h(x) \sim A_0(t)(s-x)^3 + A_1(t)(s-x)^4 + B(t)(s-x)^{8-3n} \quad \text{as} \quad x \to s^-, \tag{2.25}$$

where

$$B(t) = \frac{A_0^{1-n}\dot{s}}{(3n-4)(3n-5)(3n-6)(3n-7)(3n-8)}, \tag{2.26}$$

the three degrees of freedom being A_0, A_1 and $\dot{s}$. For $n > 4/3$ the B term intrudes in the expansion (2.25) before the second one. The expansion is admissible (i.e. the first term is indeed the leading one) if $n < 5/3$.

The locally linear solution

$$h(x) \sim A_0(t)(s-x) + A_1(t)(s-x)^2 + A_2(t)(s-x)^3 + A_3(t)(s-x)^4 + B(t)(s-x)^{6-n}, \quad \text{as} \quad x \to s^- \tag{2.27}$$

where

$$B(t) = -\frac{A_0^{1-n}\dot{s}}{(n-2)(n-3)(n-4)(n-5)(n-6)}, \tag{2.28}$$

is possible for $n < 5$ and is doubly underspecified (degrees of freedom $\dot{s}$, A_0, A_1, A_2, and A_3). Quadratic behaviour with four degrees of freedom, i.e. singly underspecified, of the form

$$h(x) \sim A_0(t)(s-x)^2 + A_1(t)(s-x)^3 + A_2(t)(s-x)^4 + B(t)(s-x)^{7-2n}, \quad \text{as} \quad x \to s^- \tag{2.29}$$

where

$$B(t) = -\frac{A_0^{1-n}\dot{s}}{(2n-3)(2n-4)(2n-5)(2n-6)(2n-7)}, \tag{2.30}$$

is possible for $n < 5/2$, the degrees of freedom being $\dot{s}$, A_0, A_1, and A_2. Finally, we have a quartic form which is singly overspecified (degrees of freedom $s(t)$ and A_0)

$$h(x) \sim A_0(t)(s-x)^4 + B(t)(s-x)^{9-4n} \quad \text{as} \quad x \to s^-, \tag{2.31}$$

https://doi.org/10.1017/S0956792504005753 Published online by Cambridge University Press

where

$$B(t) = -\frac{A_0^{1-n}\dot{s}}{(4n-5)(4n-6)(4n-7)(4n-8)(4n-9)}, \tag{2.32}$$

for $n < 5/4$.

2.5 Summary

Henceforth we shall concentrate on the correctly-specified solution branches, namely $p = 2$ for $n < 3$ and $p = 6/n$ for $3 < n < 6$ in Figure 1(a) (the $p = 6/n$ branch with $3/2 < n < 2$ can apply for suitable initial data for some finite time, but is not relevant to the large-time considerations on which we shall concentrate), $p = 3$ for $n < 2/3$ and $p = 5/(n+1)$ for $2/3 < n < 3/2$ in Figure 1(b) and $p = 3$ for $n < 5/3$ and $p = 5/n$ for $5/3 < n < 5/2$ in Figure 1(c) . We note that this excludes moving fronts for $n > 5/2$ and non-zero flux branches for $n > 3/2$, points to which we shall return later. The singly-underspecified branches are less smooth than these, but could be selected by, for example, prescribing the moment m at the interface (or, respectively, the flux $J(t)$ or the interface location $s(t)$) on the $p = 2$ branches of Figures 1(b) and 1(c) (in appropriate ranges of n, the shear force Σ or the pressure p could be specified instead), the interface location $s(t)$ (with $\dot{s} < 0$) on the $p = 5/n$ branch with $5/2 < n < 5$ in Figure 1(c), the inward flux $J(> 0)$ on the $p = 5/(n+1)$ branch with $3/2 < n < 4$ in Figure 1(b) or the contact angle $-\partial h/\partial x$ on the $p = 1$ branch of Figure 1(a); these comments can be generalised in an obvious way to the doubly-underspecified branches, which are even less smooth. The classification above is not of course exhaustive. In particular, the smoothest (correctly-specified) non-negative solution branch for the Cauchy problem with $n < 2/3$ changes rather than conserves mass, having $p = 5/(n+1)$ for $1/4 < n < 2/3$ (gaining mass) and $p = 4$ for $n < 1/4$ (gaining or losing mass); see Figure 1(b) (the front location $s(t)$ supplies the additional degree of freedom required). The fourth-order analogue to the former was identified in King & Bowen [17], but the latter represents a new phenomenon.

3 The Cauchy problem

3.1 Preliminaries

The Cauchy problem is governed by the initial conditions (1.4) and the boundary conditions (1.6). Two further conditions are required to specify the solution uniquely. Due to the degeneracy when $h = 0$ we introduce for numerical purposes a uniform thin precursor layer of positive thickness $\epsilon \ll 1$ in $|x| > s(t)$. An asymptotic analysis of the limit $\epsilon \to 0^+$ (of which we shall not report the details here for $n < 5/2$ as the results closely follow those of King & Bowen [17]) leads to the smoothest solution branch being selected (at least for n sufficiently large that film rupture does not occur). The results of §2 thus identify $n = 5/2$ as an important critical value as it separates moving fronts, $\dot{s} \neq 0$ when $n < 5/2$, from stationary ones. Consequently we first consider the regime with $0 < n < 5/2$ before examining $5/2 < n < 6$. The following table summarises the local behaviour, the fixed-front cases of course being those with $J = 0$. Note that for $n < 5/3$ the expansion

https://doi.org/10.1017/S0956792504005753 Published online by Cambridge University Press

(2.25) places no constraint on the sign of $\dot{s}$, whereas for $5/3 < n < 5/2$ we require $\dot{s} > 0$ in view of (2.24).

Range	p	$\dot{s}$
$n < \frac{5}{3}$	3	> 0 or < 0
$\frac{5}{3} < n < \frac{5}{2}$	$\frac{5}{n}$	> 0
$\frac{5}{2} < n < 3$	2	$= 0$
$3 < n < 6$	$\frac{6}{n}$	$= 0$

3.2 The moving-front regime $n < 5/2$

As already indicated, the two boundary conditions (1.6) (which define the interface and impose conservation of mass) necessarily hold here but two further conditions are needed in the sixth-order case to furnish a correctly-specified problem. In mathematical terms, there is a large number of legitimate choices for these "missing" conditions and the classification we have given in § 2 enables these to be characterised. In following our policy of investigating the smoothest-solution branches, the appropriate "missing" boundary conditions here are zero contact angle and moment, i.e. in addition to (1.6) we have

$$\text{at} \quad x = s(t) \quad \frac{\partial h}{\partial x} = \frac{\partial^2 h}{\partial x^2} = 0. \tag{3.1}$$

The large-time behaviour, for $-6 < n < 5/2$, is given by the mass preserving similarity solution (the corresponding solution for $n < -6$ exhibit finite time extinction), namely

$$h \sim t^{-1/(n+6)} f(\eta), \quad \eta = x/t^{1/(n+6)}, \quad s \sim \eta_0 t^{1/(n+6)} \quad \text{as} \quad t \to \infty \tag{3.2}$$

(see also Smyth & Hill [21] and Bernis & Friedman [3]), where f satisfies

$$-\frac{1}{n+6}\eta = f^{n-1}\frac{d^5 f}{d\eta^5}, \tag{3.3}$$

subject to

$$\begin{aligned} &\text{at } \eta = 0 \qquad \frac{df}{d\eta} = \frac{d^3 f}{d\eta^3} = 0, \\ &\text{at } \eta = \eta_0 \qquad f = \frac{df}{d\eta} = \frac{d^2 f}{d\eta^2} = 0, \end{aligned} \tag{3.4}$$

with the constant η_0 being determined by

$$\int_0^{\eta_0} f(\eta)d\eta = M/2, \tag{3.5}$$

so that η_0 is proportional to $M^{n/(n+6)}$

https://doi.org/10.1017/S0956792504005753 Published online by Cambridge University Press

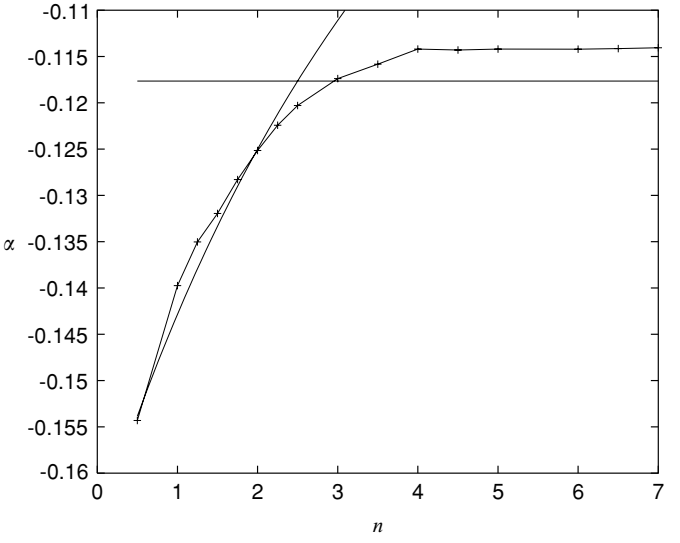


FIGURE 2. Plot of α against n, where α is a measure of the large time behaviour of the maximum height of the fluid as defined by $h = t^{\alpha} f$. Also shown are the curves $\alpha = -1/(n+6)$ and $\alpha = -2/17$ which are the predicted behaviour in § 3.2 and § 3.3.

For $n = 1$ equation (3.3) can be easily solved giving (cf. Smyth & Hill [21]; the analogous solution to the porous-medium equation (the corresponding second-order problem) is available explicitly for all n and is commonly known as the Barenblatt–Pattle solution)

$$f = \frac{1}{7!}\left(\eta_0^2 - \eta^2\right)^3, \tag{3.6}$$

with the mass and η_0 related by

$$M = \frac{1}{7!}\frac{32}{35}\eta_0^7.$$

For $n = 2$ the first integral

$$\frac{1}{16}\left(\eta_0^2 - \eta^2\right) = f\frac{d^4 f}{d\eta^4} - \frac{df}{d\eta}\frac{d^3 f}{d\eta^3} + \frac{1}{2}\left(\frac{d^2 f}{d\eta^2}\right)^2$$

is available.

Numerical solutions illustrating the above behaviour are given in Figures 2, 3 and 4. A brief summary of the numerical approach adopted is given in the Appendix. In these numerical results we use the initial conditions (with $a = 2$)

$$h(x,0) = \begin{cases} (1-\epsilon)\left(1 - \frac{1}{4}x^2\right)^3 + \epsilon & \text{in } |x| < 2, \\ \epsilon \quad \text{in} \quad |x| \geqslant 2, \end{cases} \tag{3.7}$$

with $\epsilon = 0.01$ (we recall that it can be shown that such a prewetting regularisation selects in the asymptotic limit $\varepsilon \to 0$ the boundary conditions (3.1), at least if film rupture does not occur). Given the delicacy of this problem numerically, Figure 2 provides reasonable

https://doi.org/10.1017/S0956792504005753 Published online by Cambridge University Press

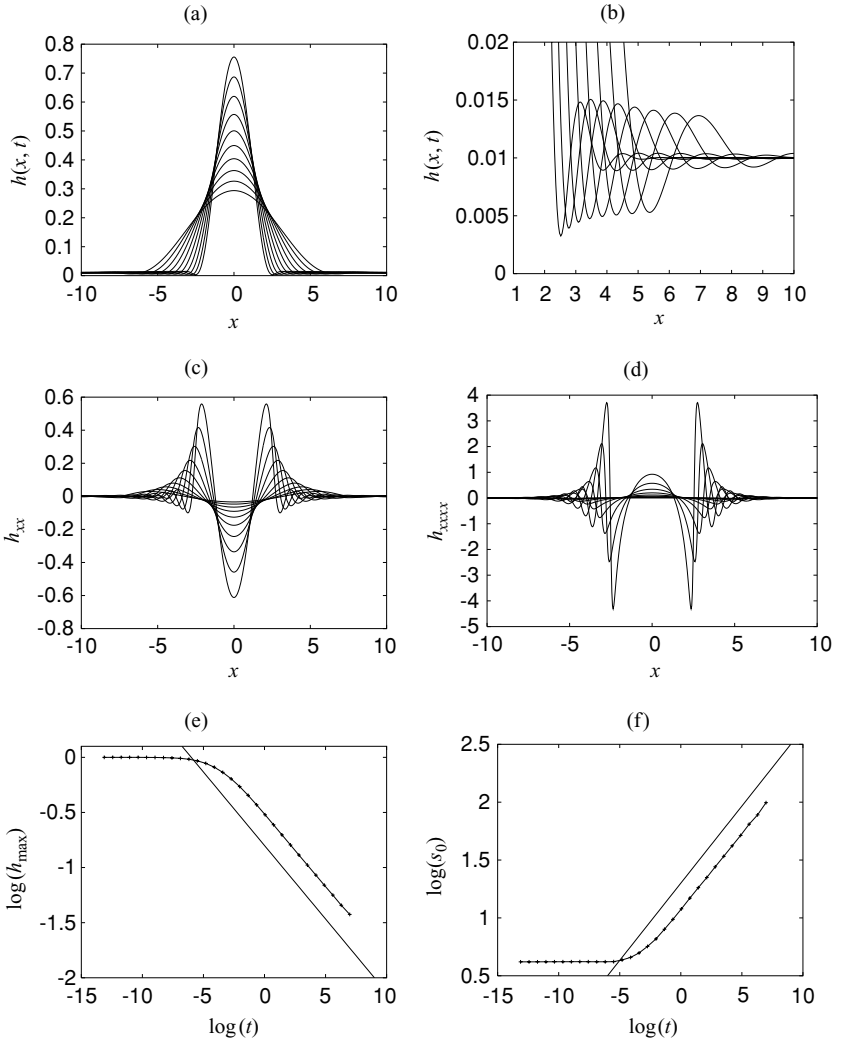


FIGURE 3. Solution plots for the Cauchy problem for $n = 1.5$. Plotted are a range of typical height profiles, (a), with a close up on the front behaviour, (b), the curvature ($= h_{xx}$), which determines the bending moment in the beam, and the pressure ($= h_{xxxx}$), along with log-log plots of the maximum height and front position. In the log-log plots the straight lines correspond to the curve $t^{\pm 2/15}$ as appropriate (see (3.2)). We define the front, s_0, as the point where $h = 2\epsilon$. The high pressures that exist around the leading edge of the drop are noteworthy; such effects can be of importance in applications since they may, for example, cause the plate to separate from the fluid film and the substrate; we shall not, however, investigate such phenomena here.

support for the asymptotic results. The exponent α is estimated by plotting $\log h_{\max}$ against $\log t$ and determining the slope by fitting a straight line over the "large-time" regime.

A feature which has attracted significant interest in the fourth-order case (see, for example, Bertozzi [5]) is the issue of film rupture, whereby h spontaneously develops a

https://doi.org/10.1017/S0956792504005753 Published online by Cambridge University Press

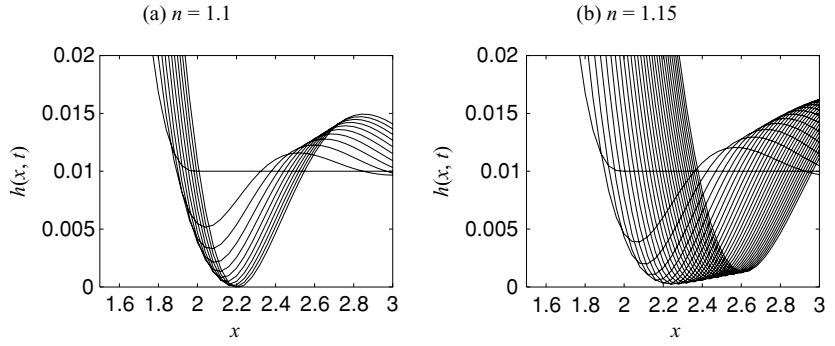


FIGURE 4. Close up views of the front for the Cauchy problem demonstrating finite time break off of solutions. (a) A range of profiles up until break off for $n = 1.1$, with (b) an equivalent set of pictures for $n = 1.15$ where break off does not occur.

zero from strictly positive initial data. The small ϵ asymptotics show that such break off necessarily occurs for $n < 2/3$ (the critical case corresponds to the solution branches $p = 3$ and $p = 5/(n+1)$ coinciding; in the fourth-order case we instead have $n < 1/2$, the upper limit having $2 = 3/(n+1)$ see King & Bowen [17]); for $n > 2/3$ an interior zero will not be present at a front advancing over a thin pre-wetting layer, but the fact that retreating fronts can occur when $n < 5/3$ suggests that this may play a role in determining the upper bound for rupture (the corresponding exponent for the fourth-order equation is $n = 3/2$ and issues relating to the precise value of the critical exponent remain open in that case also). We shall not attempt to analyse such matters further here, but include as an illustrative plot Figure 4, which suggests rupture occurs when $n = 1.1$ with initial conditions given in (3.7); also shown is a plot for $n = 1.15$ showing the solution just failing to touch down.

3.3 $5/2 < n < 6$

We saw in §2 that for $n > 5/2$ the smoothest solutions have fixed fronts, being given by the solid branches in Figure 1(a) in $n > 5/2$ and transferring in a continuous fashion onto the solid branch in Figure 1(b) at $n = 5/2$. The "missing" boundary conditions are thus $\dot{s} = 0$ (i.e. $s = a$) and

$$\text{at} \quad x = a \quad \frac{\partial h}{\partial x} = 0, \tag{3.8}$$

in addition to (1.6). Consequently we expect the solution to tend, as $t \to \infty$ to the steady-state solution

$$h = \frac{15M}{16a}\left(1 - \frac{x^2}{a^2}\right)^2 \quad \text{for} \quad |x| < a. \tag{3.9}$$

Figure 5 shows log-log plots of the height profile near the front, in order to assess consistency with the local behaviour postulated in the table above. Specifically, we plot $\log(h - \epsilon)$ against $\log(s_0 - x)$ i.e. we translate off the precursor film and shift the frame to the front (numerically we again take the "front" (s_0) to be the point where $h = 2\epsilon$). The behaviours $x^{6/n}$ and x^2 are also shown, agreement between the numerical and analytical

https://doi.org/10.1017/S0956792504005753 Published online by Cambridge University Press

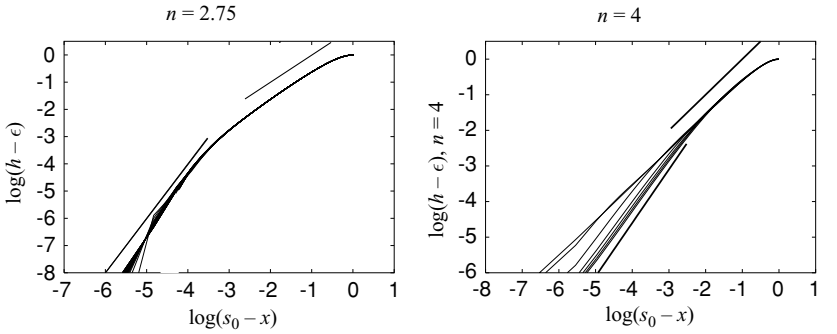


FIGURE 5. Log log plots of the behaviour near the front for the Cauchy problem when in the 'fixed' front regime. Also plotted are (thicker) straight lines corresponding to (lower line) front behaviour of the form x^2 in the left-hand plot (lying in the regime $5/2 < n < 3$) and $x^{6/n}$ in the right-hand plot (lying in the regime $3 < n < 6$), with which the agreement improves as t increases, and to (upper line) x^1 (i.e. to the local behaviour near $x = a$ of the initial conditions).

solutions in general being good, given that the local singularities receive no special numerical treatment.

For $t = O(1)$ no interface motion occurs and the solution evolves to (3.9), the numerical results for $t = O(1)$ being consistent with these assertions; see Figure 6. However, when a thin prewetting layer is present there is a longer timescale $T = \epsilon^{n-5/2}t$ in which the outer solution is quasi-steady,

$$h \sim \frac{15M}{16s_0(T)}\left(1 - \frac{x^2}{s_0^2(T)}\right)^2 \quad |x| < s_0(T) \tag{3.10}$$

and the film slowly spreads out. The details of how s_0 is obtained are worth spelling out briefly (see King [14] for more details), in part because the Newtonian case $n = 3$ lies within this regime. Thus, the inner scalings are

$$x = s(T;\epsilon) + \epsilon^{1/2}z, \quad h = \epsilon g$$

where $s(T;0) = s_0(T)$ and

$$\begin{aligned} &-\dot{s}_0(g_0 - 1) = g_0^n \frac{\partial^5 g_0}{\partial z^5} \\ &\text{as} \quad z \to +\infty \quad g_0 \to 1 \\ &\text{as} \quad z \to -\infty \quad g_0 \to \Omega(T)(-z)^2 \end{aligned} \tag{3.11}$$

where $\dot{s}_0 = ds_0/dT$ and Ω is determined as part of the solution to (3.11), which specifies g_0 up to translations of z; it is the need to obtain a travelling-wave balance here that identifies the long timescale $T = O(1)$. Since

$$g_0 = g_0\left(\dot{s}_0^{1/5}z\right)$$

it follows that

$$\Omega = \beta(n)\dot{s}_0^{2/5}$$

for some constant β whose value can be determined only by solving (3.11) numerically.

https://doi.org/10.1017/S0956792504005753 Published online by Cambridge University Press

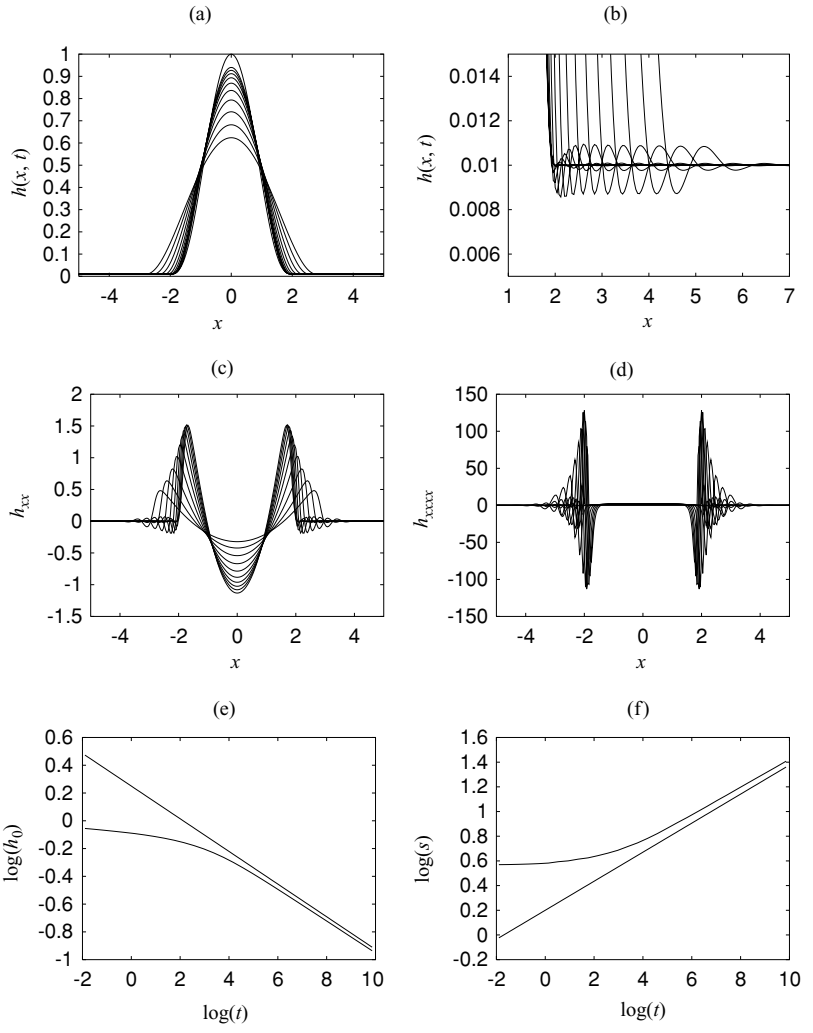


FIGURE 6. Solution plots for the Cauchy problem for $n = 4$. Plotted are a range of typical height profiles, (a), with a close up on the front behaviour, (b), the curvature ($= h_{xx}$) and the pressure ($= h_{xxxx}$), along with log-log plots of the maximum height and front position. In the log-log plots the straight lines correspond to the curve $t^{\pm 2/17}$ as appropriate (see (3.13)–(3.14)). Again, we note the high pressures at the leading edge, these being much larger than for $n = 1.5$.

Matching to (3.10) then requires

$$\beta \dot{s}_0^{2/5} = \frac{15M}{4s_0^3} \tag{3.12}$$

so that

$$s_0 = \left(a^{17/2} + \frac{3825\sqrt{15}}{64} \left(\frac{M}{\beta} \right)^{5/2} T \right)^{2/17}. \tag{3.13}$$

More generally, (3.12) corresponds to a moving-boundary condition

$$\text{at} \quad x = s(T) \quad \frac{\partial^2 h}{\partial x^2} = 2\beta \dot{s}^{2/5}$$

https://doi.org/10.1017/S0956792504005753 Published online by Cambridge University Press

which is the sixth-order analogy of the zero static contact angle Tanner law

$$\text{at} \quad x = s(T) \quad \frac{\partial h}{\partial x} = -\alpha \dot{s}^{1/3}$$

which arises in the fourth-order case (the corresponding condition holds also in the higher-dimensional case, leading to an interesting class of moving-boundary problems). In view of (3.13), the large-time behaviour can be characterised by the self-similar form

$$h \sim T^{-2/17} F\big(x/T^{2/17}\big); \tag{3.14}$$

again see Figure 2, which summarises the large-time behaviour. While the above results (in particular (3.13)) can be expected to apply also for $n > 6$ on the long timescale $T = O(1)$, there is a crucial gap in this case in that no plausible balance has been identified which describes the behaviour for $t = O(1)$. We return to this matter in detail in § 6.

The above scenario holds for $n = 4$, which we use to demonstrate this behaviour numerically. We solve (1.1) using the numerical approach summarised in the Appendix for initial data given in (3.7). Figure 6 shows typical height profiles for $n = 4$ along with a close up of the front behaviour. Also shown are log-log plots of the maximum height and front position over time. The log-log plots provide convincing evidence that the behaviour of the maximum height and front indeed follow the predictions above.

4 Fixed domain

4.1 Formulation

For the fixed domain problem (with $|x| < a$) we have (1.7) and § 2 determines $n = 3/2$ as the key critical value, revealing that the smoothest solution branches have

$$\text{at} \quad x = a \quad \frac{\partial h}{\partial x} = \frac{\partial^2 h}{\partial x^2} = 0 \tag{4.1}$$

as the missing boundary conditions for $n < 3/2$ and

$$\text{at} \quad x = a \quad \frac{\partial h}{\partial x} = h^n \frac{\partial^5 h}{\partial x^5} = 0 \tag{4.2}$$

for $n > 3/2$. The local behaviour of the solutions is summarised in the following table.

Range	p	J
$n < \frac{2}{3}$	3	> 0 or < 0
$\frac{2}{3} < n < \frac{3}{2}$	$\frac{5}{n+1}$	< 0
$\frac{3}{2} < n < 3$	2	$= 0$
$3 < n < 6$	$\frac{6}{n}$	$= 0$

https://doi.org/10.1017/S0956792504005753 Published online by Cambridge University Press

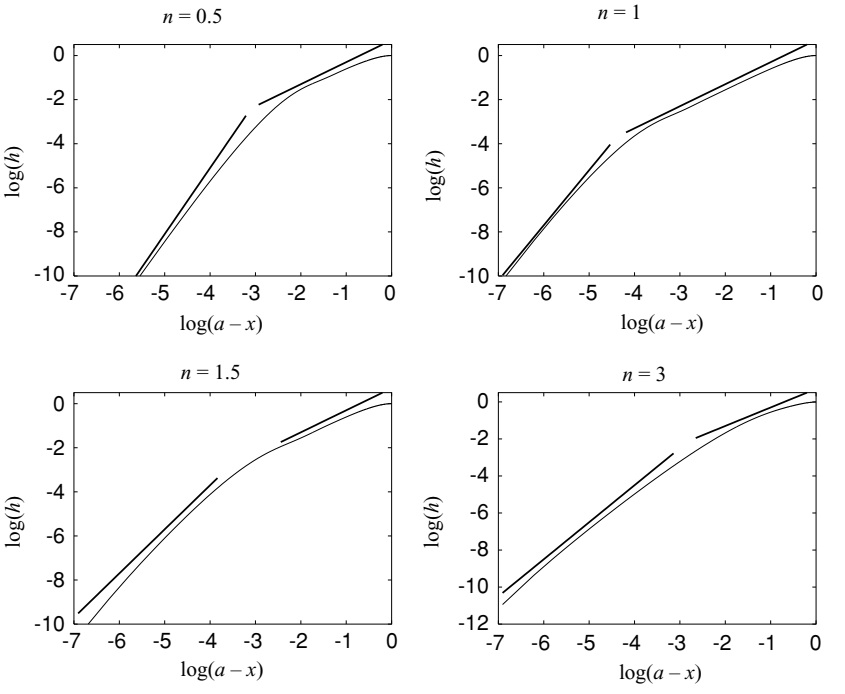


FIGURE 7. Log-log plots of the behaviour near the boundary for the fixed domain problem. In each plot a numerical solution is shown along with straight lines corresponding to the predicted local behaviour and the linear behaviour that corresponds to the initial profile (the latter being the higher, shallower line in each plot).

Thus for $3/2 < n < 6$ there is no fluid loss while in $2/3 < n < 3/2$ only drainage is possible. Both out-flow ($J < 0$) and in-flow of fluid ($J > 0$) are possible for $n < 2/3$ and the latter is undesirable in the context in which the formulation most naturally applies (see Bowen & King [6] for discussion of the corresponding fourth-order regime $n < 1/2$). Figure 7 shows log-log plots of the fluid height against $a - x$ for $n = 0.5, 1, 1.5, 2, 3$ and 4. The initial conditions used were (with $a = 1$)

$$h(x, 0) = \cos\left(\frac{\pi x}{2}\right) \quad \text{in } |x| \leqslant 1. \tag{4.3}$$

The agreement is good for all values of n.

4.2 $0 < n < 3/2$

In this regime we have infinite-time extinction (finite-time extinction occurs for $n < 0$) and the large-time behaviour is given by the separable solution

$$h \sim t^{-1/n} f(x), \tag{4.4}$$

which implies in particular that the mass of fluid ultimately decays as $t^{-1/n}$ (for $n = 0$ the decay is exponential and the separable solution can be constructed explicitly). The

https://doi.org/10.1017/S0956792504005753 Published online by Cambridge University Press

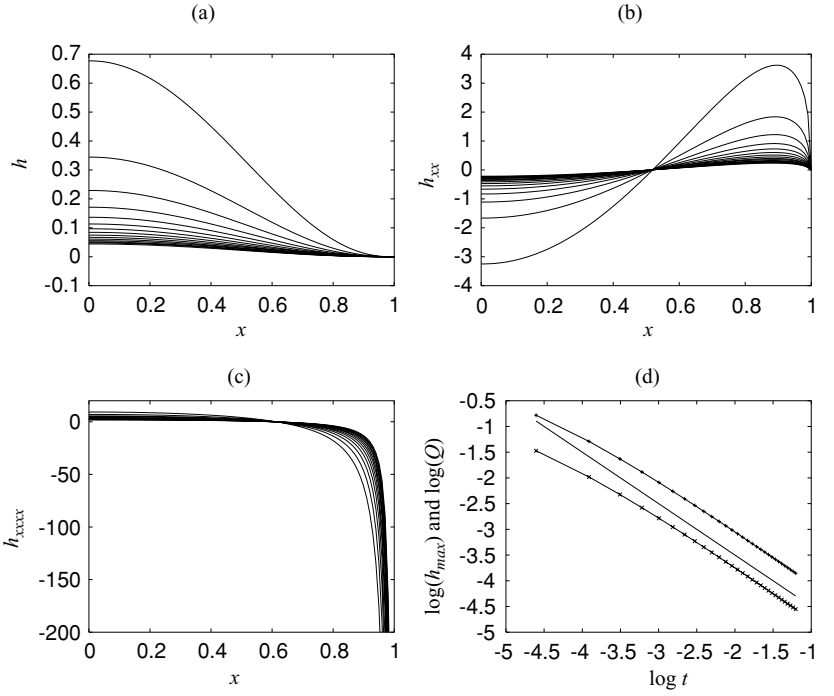


FIGURE 8. Fixed-domain solutions for $n = 1$. Plot of (a) height profiles over time, (b) the curvature (h_{xx}), (c) the pressure (h_{xxxx}), and (d) a log-log plot of maximum height and mass against time; (d) also shows the predicted large-time behaviour, i.e. $h, Q \sim t^{-1/n}$ ($\log(h_{\max})$ is the lowest curve and $\log Q(t)$ the top one, $Q(t)$ being the time varying mass defined in (4.6)). The mass drains at a rate that matches the theoretical prediction. Note, as in the Cauchy case, the large pressures at the draining boundary, which could have significant implications in practice.

boundary-value problem for f is then

$$\begin{aligned} &-\frac{1}{n}f = \frac{d}{dx}\left(f^n \frac{d^5 f}{dx^5}\right), \\ &\text{at} \quad x = 0 \quad \frac{df}{dx} = \frac{d^3 f}{dx^3} = \frac{d^5 f}{dx^5} = 0, \\ &\text{at} \quad x = a \quad f = \frac{df}{dx} = \frac{d^2 f}{dx^2} = 0. \end{aligned} \tag{4.5}$$

Figure 8 shows a range of plots for $n = 1$, imposing (4.1). The mass decreases in this regime and we define

$$Q(t) = \int_{-a}^{a} h(x,t)dx. \tag{4.6}$$

For comparison we also solve for constant-mass boundary conditions (4.2) (note that the relevant branch in Figure 1(a) is present for $n < 3/2$ but is less smooth than the "drainage" branch in Figure 1(b)), the results shown in Figure 9 being indicative of constant mass solutions in a fixed domain. As $t \to \infty$ the solution tends to a steady state that matches well with the predicted profile.

https://doi.org/10.1017/S0956792504005753 Published online by Cambridge University Press

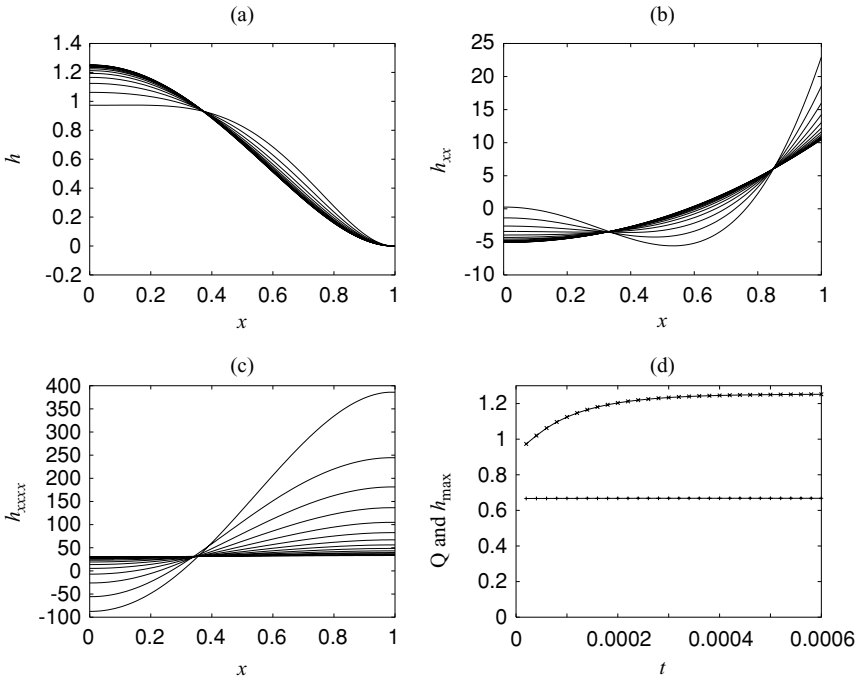


FIGURE 9. Fixed-domain solutions for $n = 1$ with constant mass. Plot of (a) various height profiles over time, (b) the curvature (h_{xx}), (c) the pressure (h_{xxxx}), and (d) a plot of maximum height (upper curve) and mass (lower curve) against time. These plots are to be compared with Figure 8 where the boundary conditions allow drainage, the difference in the pressure plots being particularly noteworthy.

4.3 $3/2 < n < 6$

In this range of n the smoothest solutions correspond to zero-flux boundary conditions which have already been touched on in § 3.3. Throughout this range the solution tends to the steady state (3.9) and we do not need to discuss this case further. Figure 10 summarises the asymptotic behaviour of the smoothest solutions of the finite domain problem.

5 "Dipole" problem

5.1 Preamble

The dipole problem can be regarded as a combination of the previous two boundary value problems. Here we have boundary conditions of the fixed domain type at the left-hand boundary, the conditions at the right-hand boundary being the same as for the Cauchy problem.

We summarise the local behaviour at both boundaries in the following table. There are now two main transitions, one (at $n = 3/2$) that separates constant and varying mass solutions and one (at $n = 5/2$) that separates moving and fixed front solutions.

https://doi.org/10.1017/S0956792504005753 Published online by Cambridge University Press

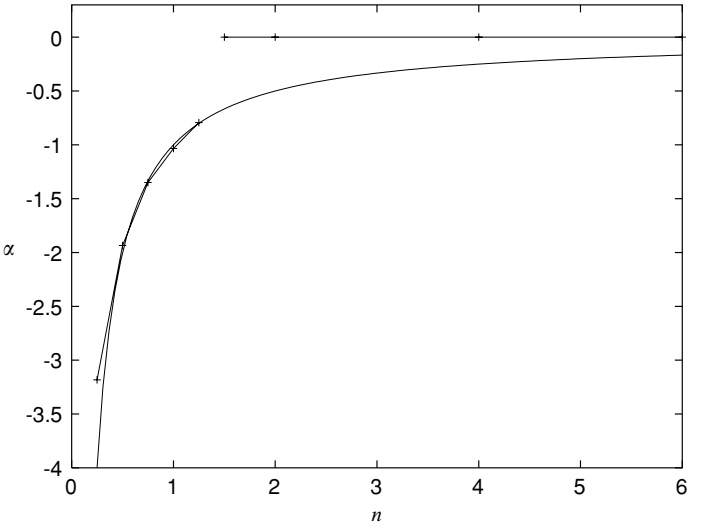


FIGURE 10. The power-law behaviour of the maximum height of fluid, defined via $h \sim t^{\alpha} f(x)$, against n in a fixed domain. The value of α is found using the method outlined in § 3.2. There is a transition at $n = 3/2$ above which the solutions conserve mass and a steady state results. Also shown is the curve $\alpha = -1/n$, which matches well with the numerical solution below $n = 3/2$. For $n > 3/2$ we find $\alpha = 0$. Numerically we impose (4.1) in $n < 3/2$ and (4.2) $n > 3/2$. There is thus an abrupt change in the exponent at $n = 3/2$, though as n approaches $3/2$ from below the flux out of the domain tends to zero within the self-similar formulation (4.4)–(4.5).

Range	left boundary p	J	right boundary p	$\dot{s}$
$n < \frac{2}{3}$	3	> 0 or < 0	3	> 0 or < 0
$\frac{2}{3} < n < \frac{3}{2}$	$\frac{5}{n+1}$	< 0	3	> 0 or < 0
$\frac{3}{2} < n < \frac{5}{3}$	2	$= 0$	3	> 0 or < 0
$\frac{5}{3} < n < \frac{5}{2}$	2	$= 0$	$\frac{5}{n}$	> 0
$\frac{5}{2} < n < 3$	2	$= 0$	2	$= 0$
$3 < n < 6$	$\frac{6}{n}$	$= 0$	$\frac{6}{n}$	$= 0$

For $n > 5/2$ we have a zero-flux fixed-front conditions on both boundaries so this case has already been addressed, the large-time behaviour being the steady-state (3.9). For $3/2 < n < 5/2$ we have a zero-flux condition at $x = 0$ and a moving boundary ($\dot{s} > 0$) on the right-hand side. In this regime the similarity solution given in (3.2) is applicable at large time though the conditions on $\eta = 0$ in (3.4) are replaced by

$$\text{at} \quad \eta = 0 \qquad f = \frac{df}{d\eta} = f^n \frac{d^5 f}{d\eta^5} = 0;$$

the similarity solution is again available in closed form for $n = 1$. Consequently, we will

https://doi.org/10.1017/S0956792504005753 Published online by Cambridge University Press

concentrate our analysis in this section on $n < 3/2$ as the behaviour in this range of n differs significantly from that described in the previous two sections.

5.2 $n < 3/2$

We assume a similarity solution of the form

$$h \sim t^{\alpha} f(\eta), \quad \eta = x/t^{\beta}, \quad s = \eta_0 t^{\beta} \quad \text{as} \quad t \to \infty \tag{5.1}$$

where $-n\alpha + 6\beta = 1$ and f satisfies

$$\alpha f - \beta\eta \frac{df}{d\eta} = \frac{d}{d\eta}\left(f^n \frac{d^5 f}{d\eta^5}\right). \tag{5.2}$$

The mass of fluid decreases according to

$$Q(t) = \int_0^{\infty} h dx \sim t^{\beta+\alpha} \int_0^{\infty} f d\eta \quad \text{as} \quad t \to \infty$$

as it drains through $x = 0$. It thus follows that $-\alpha > \beta$ but, as in the fourth-order case [4], the value of the exponent α is in general determined by the nonlinear eigenvalue problem for $f(\eta)$; in other words, (5.1) is a similarity solution of the second kind.

For $n = 1$, however, we can obtain an additional conservation law by observing that equation (1.1) is then identical to

$$\frac{\partial h}{\partial t} = \frac{\partial^2}{\partial x^2}\left(h\frac{\partial^4 h}{\partial x^4} - \frac{\partial h}{\partial x}\frac{\partial^3 h}{\partial x^3} + \frac{1}{2}\left(\frac{\partial^2 h}{\partial x^2}\right)^2\right),$$

implying that the first moment

$$\int_0^{s(t)} x h dx = M_1$$

is independent of time, since h, $\partial h/\partial x$ and $\partial^2 h/\partial x^2$ are all zero at both $x = 0$ and $x = s(t)$. This implies that $2\beta + \alpha = 0$ and hence that $\alpha = -1/4$ and $\beta = 1/8$ in this special case.

5.3 Numerical solution

5.3.1 *Formulation*

We compute the solution numerically for a range of n. At the left-hand boundary, $x = 0$, we impose two different sets of boundary conditions depending on the value of n. For $n < 3/2$, there are the drainage conditions

$$\text{at} \quad x = 0 \quad h = \frac{\partial h}{\partial x} = \frac{\partial^2 h}{\partial x^2} = 0, \tag{5.3}$$

while for $n > 3/2$ we have mass conservation,

$$\text{at} \quad x = 0 \quad h = \frac{\partial h}{\partial x} = h^n \frac{\partial^5 h}{\partial x^5} = 0. \tag{5.4}$$

https://doi.org/10.1017/S0956792504005753 Published online by Cambridge University Press

It is clear from Figure 1(a) that the conditions (5.4) can also be applied in $n < 3/2$, whereas from Figure 1(b) we cannot impose (5.3) in $n > 3/2$. To illustrate this we show in Figure 11 numerical solutions for $n = 1$ with both sets of conditions. The initial conditions used in these simulations are parabolic

$$\text{at } t=0 \quad h=1-(x-1)^2 \quad \text{in} \quad 0<x\leqslant(1-\epsilon)^{1/2}+1, \quad h=\epsilon \quad \text{in} \quad x>(1-\epsilon)^{1/2}+1. \tag{5.5}$$

These plots demonstrate the spreading behaviour at the moving boundary and also confirm the postulated large-time behaviour in both cases.

5.3.2 *Exponents α for various n*

From the numerical solutions we calculate the approximate large-time dependence of α on n and plot them in Figure 12. Two solid lines are included, the curved line is $\alpha = -1/(n+6)$, as predicted for constant mass spreading behaviour, and the second is a straight line at $\alpha = -2/17$ which corresponds to the quasi-steady behaviour that occurs with prewetting for $n > 5/2$. The plot of α against n gives rough numerical estimates for the second-kind behaviour which occurs for $n < 3/2$, as well as concurring elsewhere with the analytical predictions.

6 $n > 6$

6.1 Preamble

The table of regimes in § 5 stops at $n = 6$, reflecting the fact that we have yet to identify legitimate solution branches for $n \geqslant 6$. As already indicated, for sufficiently large n (i.e. for $n > 5/2$) we expect no interface motion on the smoothest solution branch so, to conserve mass, we require

$$\text{at } x = \pm a \quad h = h^n \frac{\partial^5 h}{\partial x^5} = 0,$$

leaving, as usual, a single boundary condition missing. Moreover, it is clear that the separable solution ((2.2)–(2.3) with $p = 6/n$) cannot describe the local behaviour for $n > 6$ (we stress there is no analogous regime for the corresponding fourth-order case, with the separable solution then holding for all $n > 4$). Our procedure here is to build up understanding by considering different local forms for the initial conditions, $h_i(x)$, which for brevity we again take to be symmetric in x. For definiteness, we assume

$$h_i(x) \sim A(a-x)^p \quad \text{as } x \to a^-. \tag{6.1}$$

The local expansion

$$h \sim A(a-x)^p + A^{n+1}p(p-1)(p-2)(p-3)(p-4)((n+1)p-5)(a-x)^{(n+1)p-6}t \quad \text{as } x \to a^- \tag{6.2}$$

follows from (6.1) provided

$$p > \frac{6}{n} \tag{6.3}$$

https://doi.org/10.1017/S0956792504005753 Published online by Cambridge University Press

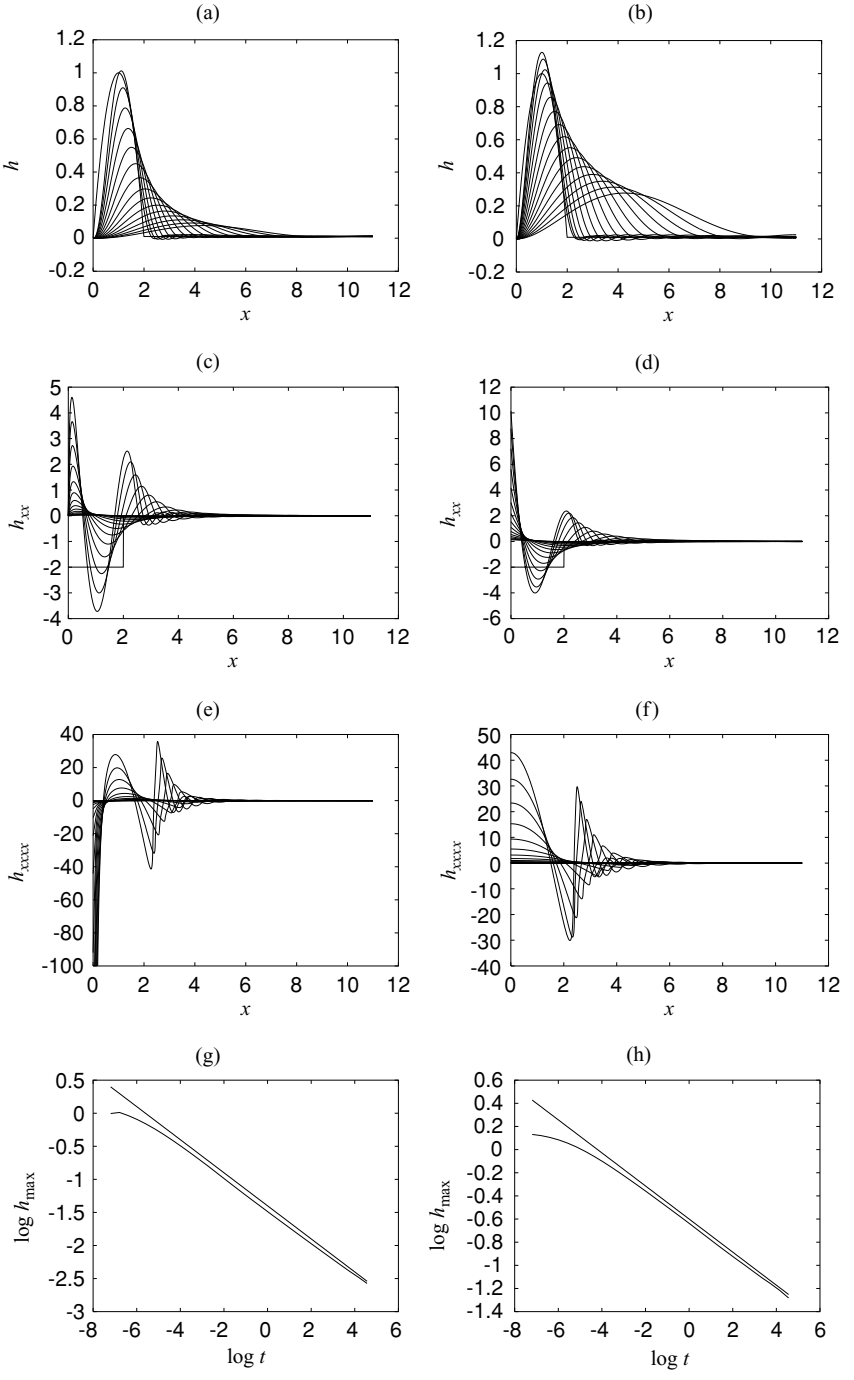


FIGURE 11. For the case $n = 1$ we plot the height, h_{xx} (the bending moment in the plate), h_{xxxx} (the pressure) and a log-log plot of $h_{\max}$ over time. In the left-hand column we impose (5.3) at $x = 0$ and in the right-hand (5.4). The predicted large time behaviour matches well in both cases, namely $t^{-1/7}$ for the mass preserving case and $t^{-1/4}$ for the draining case, the corresponding straight lines being included in the final row.

https://doi.org/10.1017/S0956792504005753 Published online by Cambridge University Press

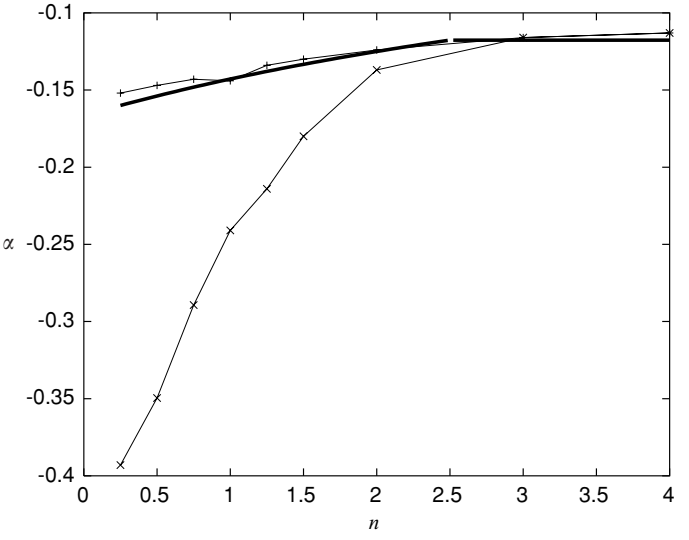


FIGURE 12. Plot of the numerical evaluated exponent α against n. The crosses are the numerically calculated values, the upper curve being the constant mass solutions and the lower those with mass loss. The straight lines are the curves $\alpha = -1/(n+6)$ and $\alpha = -2/17$. The lower curve with $n < 3/2$ corresponds to "second-kind" cases in which no explicit expression for α is available, the current (albeit rather crude) numerical estimates thus providing the only information to date about the values of the similarity exponents. The switch between branches should occur at $n = 3/2$, but is evidently deferred to somewhat larger n by the accuracy of the numerics (the time required to attain the large-time asymptotic behaviour increases around the borderline, explaining some of the discrepancy); indeed, for $n > 3/2$ on the lower curve the numerical scheme is attempting to capture a solution branch which is not in fact present.

(at least for sufficiently small time; as we shall see, it in fact holds for all time). Of course, the regime $n > 6$ is that in which the constraint (6.3) is satisfied for $p = 1$; this will prove important in what follows.

We now work down through successively decreasing ranges of p, the complexity of the problem for the most part increasing as p decreases. Some of the results are also applicable to regimes with $n < 6$.

6.2 $p > 1$

6.2.1 *Outer solution,* $x = O(1)$

As suggested by (6.2), in this range we have $\partial h/\partial x = 0$ on $x = a$ for all t and the steady-state solution

$$h = \frac{15M}{16a}\left(1 - \frac{x^2}{a^2}\right)^2 \tag{6.4}$$

can be expected to provide the large-time behaviour, at least away from the boundaries. To discuss the boundary layers we now need to sub-divide this regime into three subcases, according to the sign of $p - 2$.

https://doi.org/10.1017/S0956792504005753 Published online by Cambridge University Press

6.2.2 *Inner structure: $p > 2$*

Here we have (6.4) holding as $t \to \infty$ behind some "travelling wave" located about $x = a - s(t)$, say, with

$$h \sim \Lambda(a-x)^p \quad \text{as } t \to \infty \ \text{ for } \ (a-x)/s < 1. \tag{6.5}$$

Setting $x = a - s(t) + z$, the dominant balance takes the form

$$\begin{aligned} &\dot{s}\,(h - \Lambda s^p) \sim h^n \frac{\partial^5 h}{\partial z^5}, \\ &\text{as} \quad z \to +\infty \quad h \to \Lambda s^p, \\ &\text{as} \quad z \to -\infty \quad h \sim \frac{15M}{4a^3}(-z)^2 \end{aligned} \tag{6.6}$$

where we have matching with (6.5) and (indirectly) with (6.4) (in a transition region $a - x = O(s)$ with $(a-x)/s > 1$, the leading-order solution takes the quasi-steady form $h \sim 15M(s-x)^2/4a^3$).

Given that $\dot{s} < 0$, in (6.6) we have two boundary conditions as $z \to +\infty$ (since the two exponentially growing terms in the linearisation about Λs^p must be suppressed) and three as $z \to -\infty$ (the two degrees of freedom left being the $(-z)^1$ and $(-z)^0$ terms). Since the fifth-order boundary value problem (6.6) determines h only up to transitions of z, these five boundary conditions serve in effect to determine $s(t)$ as part of the solution. Thus setting

$$h = \Lambda s^p H(Z), \quad z = ((\Lambda s^p)^n/(-\dot{s}))^{1/5} Z \tag{6.7}$$

we obtain

$$\begin{aligned} &H^n \frac{\partial^5 H}{\partial Z^5} = -(H-1), \\ &\text{as} \quad Z \to +\infty \quad H \to 1, \\ &\text{as} \quad Z \to -\infty \quad H \sim K(-Z)^2; \end{aligned} \tag{6.8}$$

the constant $K > 0$ is determined as part of the solution to (6.8) and, by comparison with (6.6), s is then given via

$$K\Lambda s^p = \frac{15M}{4a^3}\left(\frac{(\Lambda s^p)^n}{(-\dot{s})}\right)^{2/5}$$

so that

$$s \sim \left(\frac{1}{2}\left((2n-5)p-2\right)\Lambda^{(2n-5)/2}\left(\frac{15M}{4Ka^3}\right)^{\frac{5}{2}}\right)^{-\frac{2}{(2n-5)p-2}} t^{-\frac{2}{(2n-5)p-2}} \quad \text{as } t \to \infty. \tag{6.9}$$

We note from (6.7) that z scales as $t^{-p/((2n-5)p-2)}$ so the balance is indeed self-consistent (i.e. $s \gg z$) for $p > 2$.

https://doi.org/10.1017/S0956792504005753 Published online by Cambridge University Press

6.2.3 *Inner structure: $p = 2$*

Here we have

$$h \sim t^{-\frac{1}{n-3}}\phi\big((a-x)t^{\frac{1}{2(n-3)}}\big) \quad \text{as} \quad t \to \infty \quad \text{with} \quad a - x = O\big(t^{-\frac{1}{2(n-3)}}\big), \tag{6.10}$$

with $\phi(\eta)$ given by

$$\begin{aligned} -\frac{1}{2(n-3)}\left(2\phi - \eta\frac{d\phi}{d\eta}\right) &= \frac{d}{d\eta}\left(\phi^n\frac{d^5\phi}{d\eta^5}\right), \\ \text{as} \quad \eta \to 0^+ \quad \phi &\sim \Lambda\eta^2, \\ \text{as} \quad \eta \to +\infty \quad \phi &\sim \frac{15M}{4a^3}\eta^2. \end{aligned} \tag{6.11}$$

If $\Lambda = 15M/4a^3$ then the solution is simply $\phi = 15M\eta^2/4a^3$. We note that there is continuity in the exponents characterising the time dependence between (6.7), (6.9) and (6.10) as p drops to two.

6.2.4 *Inner structure: $1 < p < 2$*

Two narrow regions near $x = a$ are now required to attain consistency with (6.2), the narrower of which (the inner-inner) having

$$h \sim t^{-\frac{p}{np-6}}\phi\big((a-x)t^{\frac{1}{np-6}}\big) \quad \text{as} \quad t \to \infty \quad \text{with} \quad a - x = O\big(t^{-\frac{1}{np-6}}\big)$$

(cf. (6.10)) with $\phi(\eta)$ given by

$$\begin{aligned} -\frac{1}{np-6}\left(p\phi - \eta\frac{d\phi}{d\eta}\right) &= \frac{d}{d\eta}\left(\phi^n\frac{d^5\phi}{d\eta^5}\right), \\ \text{as} \quad \eta \to 0^+ \quad \phi &\sim \Lambda\eta^p, \\ \text{as} \quad \eta \to +\infty \quad \phi &\sim \kappa\eta, \end{aligned} \tag{6.12}$$

where the constant κ is to be determined as part of the solution (the three degrees of freedom in (6.12) as $\eta \to 0^+$ are exponentially small, whereas as $\eta \to +\infty$ there are, in addition to κ, terms in η^0 and η^{5-n} (similar comments apply to (6.11) above, where the degrees of freedom as $\eta \to +\infty$ are terms in η^1, η^0 and η^{5-2n}); the constraint $n > 6$ is required for the far-field condition in (6.12) to represent a self-consistent balance). The inner region is quasi-steady, having

$$h \sim t^{-\frac{2(p-n)}{np-6}}\psi\big((a-x)t^{\frac{p-1}{np-6}}\big),$$

with

$$\psi(\xi) = \kappa\xi + \frac{15M}{4a^3}\xi^2.$$

https://doi.org/10.1017/S0956792504005753 Published online by Cambridge University Press

6.3 $p = 1$

6.3.1 *Asymptotic calculation*

Given, via (6.2), that $\partial h/\partial x = -\Lambda$ now holds on $x = a$ for all t, the steady-state solution (6.4) generalises to

$$h = \frac{1}{16a}\left(1 - \frac{x^2}{a^2}\right)\left(15M\left(1 - \frac{x^2}{a^2}\right) - 2a^2\Lambda\left(1 - \frac{5x^2}{a^2}\right)\right) \tag{6.13}$$

and this provides a uniformly valid representation of the large-time behaviour provided that it is positive for all $|x| < a$, i.e. provided $\Lambda < 15M/2a^2$. There turn out to be two further regimes in Λ. For $15M/2a^2 \leqslant \Lambda < 10M/a^2$ the appropriate conditions on the steady state (for reasons which follow from the inner analysis below) are that

$$\text{at} \quad x = 0 \quad h = \frac{dh}{dx} = 0,$$

giving

$$h = \frac{1}{2a}\left(1 - \frac{|x|}{a}\right)\frac{x^2}{a^2}\left(30M\left(1 - \frac{|x|}{a}\right) - \Lambda a^2\left(3 - \frac{5|x|}{a}\right)\right); \tag{6.14}$$

the constraint that $\Lambda < 10M/a^2$ corresponds to the requirement that (6.14) be positive near $x = 0$. The apparent non-analyticity of (6.14) is smoothed over an inner region

$$h \sim t^{-\frac{1}{n-3}}\Phi\left(xt^{\frac{1}{2(n-3)}}\right) \quad \text{as} \quad t \to \infty \quad \text{with} \quad a - x = O\left(t^{-\frac{1}{2(n-3)}}\right)$$

with $\Phi(\eta) > 0$ given by

$$-\frac{1}{2(n-3)}\left(2\Phi - \eta\frac{d\Phi}{d\eta}\right) = \frac{d}{d\eta}\left(\Phi^n\frac{d^5\Phi}{d\eta^5}\right),$$

$$\text{at} \quad \eta = 0 \quad \frac{d\Phi}{d\eta} = \frac{d^3\Phi}{d\eta^3} = \frac{d^5\Phi}{d\eta^5} = 0,$$

$$\text{as} \quad \eta \to +\infty \quad \Phi \sim \frac{3}{2a^3}(10M - \Lambda a^2)\eta^2,$$

the degrees of freedom as $\eta \to +\infty$ being terms in η^1, η^0 and η^{5-2n}. For $\Lambda = 10M/a^2$ we instead have

$$h \sim t^{-\frac{1}{n-2}}\Phi\left(xt^{\frac{1}{3(n-2)}}\right) \quad \text{as} \quad t \to \infty \quad \text{with} \quad a - x = O\left(t^{-\frac{1}{3(n-2)}}\right)$$

with

$$\Phi(\eta) = \frac{10M}{a^4}\eta^3 \quad + O(\eta) \quad \text{as} \quad \eta \to +\infty$$

the term in η^2 being excluded by higher-order matching into the outer region $x = O(1)$ (and so the degrees of freedom as $\eta \to +\infty$ are terms of the form η^1, η^0 and η^{5-3n}).

Finally, for $\Lambda > 10M/a^2$ the appropriate outer boundary conditions (again dictated by matching into the inner) are

$$\text{at} \quad x = b \quad h = \frac{dh}{dx} = \frac{d^2h}{dx^2} = 0,$$

https://doi.org/10.1017/S0956792504005753 Published online by Cambridge University Press

where $b \in (0, a)$ is to be determined as part of the steady-state solution, giving

$$h = \frac{\Lambda^{\frac{5}{2}}}{(10M)^{\frac{3}{2}}}(x-b)^3(a-x), \quad b = a - \left(\frac{10M}{\Lambda}\right)^{1/2} \tag{6.15}$$

as the limiting profile as $t \to \infty$ for $b < x < a$. There is a second outer region $|x| < b$ in which h is quasi-steady for large time, with

$$h \sim A(t)(b^2 - x^2)^2 \tag{6.16}$$

where A will be determined shortly, and an additional quasi-steady inner region about $x = b$ in which, writing $x = b + z$, we have to leading order that

$$\begin{aligned} & h^n \frac{\partial^5 h}{\partial z^5} = -J(t) \\ \text{as} \quad & z \to -\infty \quad h \sim 4Ab^2(-z)^2 \\ \text{as} \quad & z \to +\infty \quad h \sim \frac{\Lambda^2}{10M} z^3, \end{aligned} \tag{6.17}$$

where we have matched with both (6.15) and (6.16). Conservation of mass requires from (6.16) that

$$\frac{8b^5}{15}\frac{dA}{dt} = -J. \tag{6.18}$$

It follows by applying scaling arguments to (6.17) that the solution takes the form

$$h \sim \left(\frac{\Lambda^2}{10M}\right)^{-\frac{5}{3n-2}} J^{\frac{3}{3n-2}} \Psi\left(z \Big/ \left(\frac{\Lambda^2}{10M}\right)^{-\frac{n+1}{3n-2}} J^{\frac{1}{3n-2}}\right), \tag{6.19}$$

where $\Psi(\zeta)$ satisfies

$$\begin{aligned} & \Psi^n \frac{d^5\Psi}{d\zeta^5} = -1, \\ \text{as} \quad & \zeta \to -\infty \quad \Psi \sim L(-\zeta)^2, \\ \text{as} \quad & \zeta \to +\infty \quad \Psi \sim \zeta^3, \end{aligned} \tag{6.20}$$

which determines Ψ up to translations in ζ, with the constant L being determined as part of the solution (the degrees of freedom both as $\zeta \to +\infty$ and as $\zeta \to -\infty$ are ζ^2, ζ^1 and ζ^0 terms). Comparison with (6.17) reveals that

$$J \sim \left(\frac{\Lambda^2}{10M}\right)^{-(2n-3)} \left(\frac{4b^2}{L}\right)^{3n-2} A^{3n-2} \quad \text{as} \quad t \to \infty, \tag{6.21}$$

with b given by (6.15), and it then readily follows from (6.18) that

$$A(t) \propto t^{-\frac{1}{3(n-1)}} \quad \text{as} \quad t \to \infty. \tag{6.22}$$

https://doi.org/10.1017/S0956792504005753 Published online by Cambridge University Press

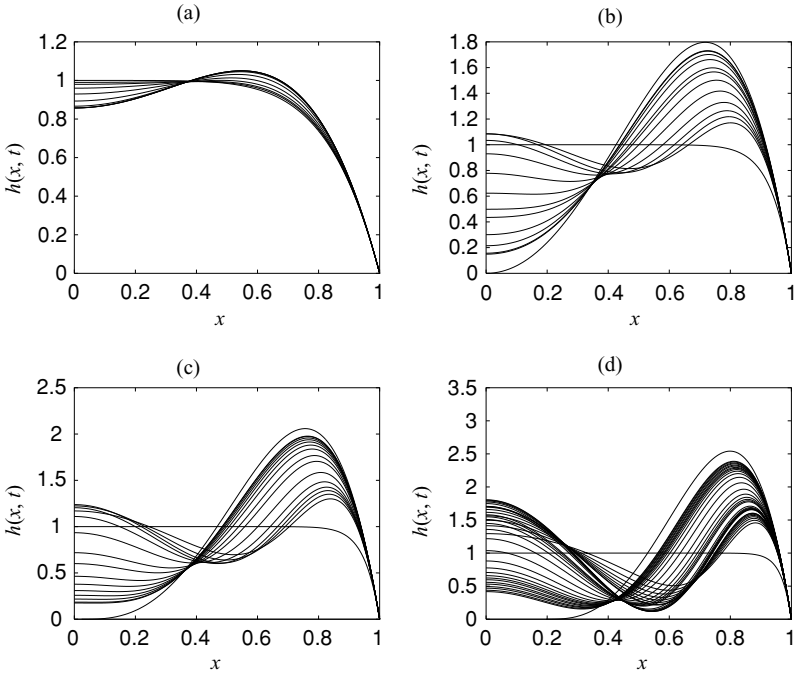


FIGURE 13. Numerical solutions to (1.1) with $n = 7$ and (a) $\Lambda = 6$, (b) $\Lambda = 15$, (c) $\Lambda = 20$ and (d) $\Lambda = 30$, illustrating the film forming a hump in the right-hand part of the domain as the plate "buckles" to a greater and greater degree (initially two humps form in $x \geqslant 0$, but the right-hand one comes to dominate the evolution).

6.3.2 *Numerical solutions*

We now consider the case $p = 1$ numerically and outline the procedure for obtaining solutions for a range of Λ. We set $a = 1$ and utilise the symmetry of the problem to solve only in positive x, and taking initial conditions of the form

$$h = 1 - x^{\Lambda} \quad \text{for} \quad 0 \leqslant x \leqslant 1, \tag{6.23}$$

consistent with (6.1). We thus impose the boundary conditions

$$\text{at} \quad x = 0 \quad \frac{\partial h}{\partial x} = \frac{\partial^3 h}{\partial x^3} = \frac{\partial^5 h}{\partial x^5} = 0, \tag{6.24}$$

$$\text{at} \quad x = 1 \quad h = 0, \quad \frac{\partial h}{\partial x} = -\Lambda, \quad \frac{\partial^5 h}{\partial x^5} = 0. \tag{6.25}$$

From (6.23) we have $M = 2\Lambda/(1 + \Lambda)$, so the three ranges of Λ that we need to consider are $\Lambda < 14$, $14 < \Lambda < 19$ and $\Lambda > 19$, corresponding to $\Lambda < 15M/2a^2$, $15M/2a^2 < \Lambda < 10M/a^2$ and $\Lambda > 10M/a^2$ respectively.

Figure 13 shows a selection of height profiles over time when we set $\Lambda = 6$, 15, 20 and 30. The corresponding steady-state solutions are also shown. In all four plots the peak height of the hump at the front (i.e. near $x = 1$) increases smoothly to the maximum

https://doi.org/10.1017/S0956792504005753 Published online by Cambridge University Press

predicted by the steady-state solutions. For $\Lambda = 15$, 20 and 30 the height near $x = 0$ increases initially before dropping as the fluid moves into the hump near $x = 1$. The figure shows clearly the tendency for large Λ for the mass to collect in a hump near the boundary. This tendency becomes much more pronounced as p drops below unity, but we have found this case numerically inaccessible owing to the unbounded first derivative at $x = a$.

6.4 $6/n < p < 1$

6.4.1 $(8n-9)/(10n-21) < p < 1$

The reason for this lower bound will remain obscure until the end of the subsection. The boundary-layer solution for $a - x = O(t^{-1/(np-6)})$ is again governed by the boundary value problem (6.12); the reason we have not needed to discuss this similarity reduction in the intervening case $p = 1$ is that its solution is then simply $\phi(\eta) = \Lambda\eta$, $\kappa = \Lambda$. Thus the matching condition

$$h \sim \kappa t^{\frac{1-p}{np-6}}(a-x) \quad \text{as} \quad x \to a^- \tag{6.26}$$

applies on "hump" region and throughout the remainder of this section we define

$$\Lambda(t) = \kappa t^{\frac{1-p}{np-6}} \tag{6.27}$$

(not to be confused with the constant Λ introduced in (6.1)) in order that we can quote unchanged expressions from the previous subsection. The "hump" thus has leading-order form (6.15) (though as we shall see below the mass M may no longer coincide with that of the initial data), where b now depends (through Λ in (6.27)) on t. Hence $b \to a$ as $t \to \infty$, so that (6.16) reduces to leading order to

$$h \sim A(t)(a^2 - x^2)^2 \tag{6.28}$$

and (6.17)–(6.21) remain valid on replacing b by a (again to leading order). In consequence, (6.22) is replaced by

$$\begin{aligned} A(t) &\propto t^{-\frac{(5n-6)p-4n}{3(n-1)(np-6)}} \quad \text{as} \quad t \to \infty \quad \text{if} \quad p > \frac{4n}{5n-6}, \\ A_\infty - A(t) &\propto t^{-\frac{4n-(5n-6)p}{(np-6)}} \quad \text{as} \quad t \to \infty \quad \text{if} \quad \frac{8n-9}{10n-21} < p < \frac{4n}{5n-6}, \end{aligned} \tag{6.29}$$

where the constant A_∞ depends on the initial data; in the second regime of (6.29) some mass remains as $t \to \infty$ in the central region (governed by (6.28)) and this is the case already alluded to in which the corresponding mass $8a^5A_\infty/15$ should be subtracted off M in the relevant expressions. In the borderline case $p = 4n/(5n-6)$, A decays logarithmically to zero as $t \to \infty$.

We can now describe how the the critical exponent $p = (8n-9)/(10n-21)$ arises. In writing down the first of (6.17), we have neglected the term $\dot{b}h$ from the convective derivative. It is readily verified from the results above that $\dot{b}h \ll J$ necessarily holds as $t \to \infty$ in the first regime of (6.29) (i.e. for $p > 4n/(5n-6)$), but in the second this self-consistency constraint can be shown to demand that $p > (8n-9)/(10n-21)$.

https://doi.org/10.1017/S0956792504005753 Published online by Cambridge University Press

6.4.2 $6/n < p < (8n-9)/(10n-21)$.

As already implied, in this case the leading-order balance (6.17) in the interior layer is replaced by

$$\begin{aligned} h^n \frac{\partial^5 h}{\partial z^5} &= -\dot{b}\,(h - h_\infty(b)), \\ \text{as} \quad z \to -\infty \quad & h \to h_\infty(b), \\ \text{as} \quad z \to +\infty \quad & h \sim \frac{\Lambda^2}{10M} z^3, \end{aligned} \tag{6.30}$$

which determines h_∞ (which at this stage is an arbitrary function of t which, for subsequent convenience, we write as a function of $b(t)$) and h up to translations in z (since $\dot{b} > 0$, the behaviour as $z \to -\infty$ contains three degrees of freedom (h_∞ and two decaying exponentials), while (translating suitably) that as $z \to +\infty$ contains two (the z^1 and z^0 terms)). Scaling arguments now give

$$\begin{aligned} h &\sim \left(\frac{\Lambda^2}{10M}\right)^{-\frac{5}{3n-5}} \dot{b}^{\frac{3}{3n-5}} \Theta\left(z \Big/ \left(\frac{\Lambda^2}{10M}\right)^{-\frac{n}{3n-5}} \dot{b}^{\frac{1}{3n-5}}\right), \\ h_\infty(b) &\sim \left(\frac{\Lambda^2}{10M}\right)^{-\frac{5}{3n-5}} \dot{b}^{\frac{3}{3n-5}} \Theta_\infty \end{aligned} \tag{6.31}$$

where $\Theta(\zeta)$ is given by

$$\begin{aligned} \Theta^n \frac{d^5\Theta}{d\zeta^5} &= \Theta - \Theta_\infty, \\ \text{as} \quad \zeta \to -\infty \quad & \Theta \to \Theta_\infty, \\ \text{as} \quad \zeta \to +\infty \quad & \Theta \sim \zeta^3, \end{aligned} \tag{6.32}$$

where the positive constant Θ_∞ is determined as part of the solution. By (6.15) we have that $\Lambda \sim 10M/(b-a)^2$ and hence, using (6.27), that

$$\dot{b} \sim \frac{1-p}{2(np-6)} \left(\frac{\kappa}{10M}\right)^{\frac{np-6}{1-p}} (a-b)^{\frac{2(np-6)}{1-p}+1};$$

we thus obtain

$$h_\infty(x) \sim \Lambda'(a-x)^{p'} \quad \text{as} \quad x \to a^-, \tag{6.33}$$

where the constants Λ' and p' are given by

$$\begin{aligned} \Lambda' &= \Theta_\infty \left(\frac{1-p}{2(np-6)}\right)^{\frac{3}{3n-5}} (10M)^{-\frac{5}{3n-5}} \left(\frac{\kappa}{10M}\right)^{\frac{3(np-6)}{(3n-5)(1-p)}}, \\ p' &= \frac{23 + 6(np-6)/(1-p)}{3n-5}. \end{aligned} \tag{6.34}$$

In $a - x = O(b)$ with $(a-x)/b < 1$, the leading-order balance is simply

$$\frac{\partial h}{\partial t} = 0$$

https://doi.org/10.1017/S0956792504005753 Published online by Cambridge University Press

subject to

$$h = h_\infty(b) \quad \text{at} \quad t = b^{-1}(x)$$

(where $^{-1}$ denotes the inverse function); thus

$$h \sim h_\infty(x)$$

pertains in this region, so (by (6.33)–(6.34)) we recover local behaviour of the form (6.1) with a new exponent p' and (in general) a new prefactor A'. The asymptotic structure outlined above therefore now recurs in $x < b$, the form it takes depending on which of the above ranges p' lies within. Self-consistency of this large-time scenario of course requires that the region closest to $x = a$ in this secondary asymptotic structure be much wider than $a - b$, so that the regions corresponding to exponent p' do not overlap with those corresponding to exponent p. It is readily shown that this is automatically the case if $p' < 2$, but if $p' > 2$ then the time dependence of (6.9) (with p replaced by p' and so on; some of the mass is taken up in the hump close to $x = a$, so the mass is also modified from that of the initial data) implies that $s \ll a - b$ (i.e. the asymptotic scenario is not self-consistent) if

$$\frac{2}{(2n-5)p'-2} > \frac{1-p}{2(np-6)}$$

which implies from (6.34) that

$$p > \frac{8n-9}{10n-21}; \tag{6.35}$$

the range in which the current analysis is admissible thus precisely complements that of the previous subsection. As p increases to the critical value in (6.35) the two travelling wave inners (6.6) and (6.30) merge, being replaced by (6.17).

This (roughly speaking) self-replicating asymptotic structure is intriguing; Figure 14 shows a schematic of this scenario. The range $6/n < p < (8n-9)/(10n-21)$ corresponds to $23/(3n-5) < p' < 8$. If $p' > 1$, which is certainly the case if $6 < n < 28/3$, then the first "repeat" follows the analysis of section 6.2 and no additional humps, and hence no further repeats, occur. However, if $p' < 1$ then additional humps will be present, as described by the preceding analysis. We note from (6.34) that the condition $p' > p$ corresponds to $p > 13/(3n-5)$, which is automatically satisfied for $p > 6/n$ with $n > 6$, so such a sequence can recur only a finite number of times, though the number of humps (which decrease in size as $a - x$ increases) can be made arbitrarily large by taking $n \to \infty$, $p \to 0$. Numerical confirmation of this result is an open problem. Our numerical scheme was unable to resolve the solution in this parameter regime.

6.5 $p = 6/n$

Obtaining comprehensive understanding of this case would require detailed analysis of the phase space of the sixth-order similarity ordinary differential equation below, so the brief results we present here should be viewed as plausible conjectures of the range of

https://doi.org/10.1017/S0956792504005753 Published online by Cambridge University Press

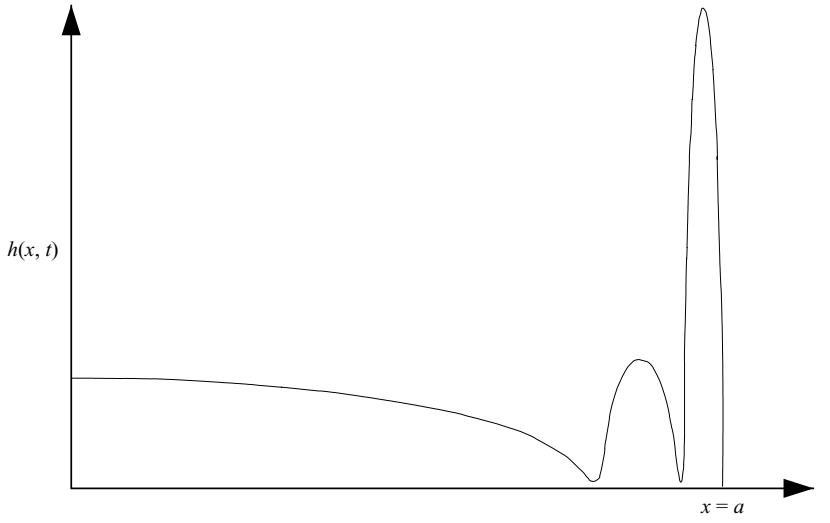


FIGURE 14. Schematic of drop with repeating humps near $x = a$.

possible behaviour. It follows from (6.1) that in this case we have

$$h \sim \left(\frac{n^5}{72(n+6)(2n-3)(n-2)(n-3)(n-6)}\right)^{\frac{1}{n}} \frac{(a-x)^{\frac{6}{n}}}{(t_c-t)^{\frac{1}{n}}} \quad \text{as} \quad x \to a^- \quad \text{for} \quad t < t_c \tag{6.36}$$

(cf. (2.3)) where

$$t_c = \left(\frac{n^5}{72(n+6)(2n-3)(n-2)(n-3)(n-6)}\right) \Lambda^{-n}$$

implying finite-time blow up of the local solution. If the first correction term to (6.1) takes the form

$$h_i \sim \Lambda(a-x)^{\frac{6}{n}} + \Omega(a-x)^{\frac{6}{n}+q} \quad \text{as} \quad x \to a^- \tag{6.37}$$

where $q > 0$ and Ω are real constants (if $\Omega \neq 0$ then we can without loss of generality scale such that $\Omega = \pm 1$) then

$$h \sim \left(\frac{n^5}{72(n+6)(2n-3)(n-2)(n-3)(n-6)}\right)^{\frac{1}{n}} \frac{(a-x)^{\frac{6}{n}}}{(t_c-t)^{\frac{1}{n}}} + \Omega t_c^{\gamma} \frac{(a-x)^{\frac{6}{n}+q}}{(t_c-t)^{\gamma}} \quad \text{as} \quad x \to a^- \tag{6.38}$$

where γ is given by

$$\begin{aligned}\gamma = \frac{n(q+1)+6}{72n(n+6)(2n-3)(n-2)(n-3)(n-6)} [n^5 q^5 + (-10\,n^5 + 30\,n^4) q^4 \\ + (35\,n^5 - 240\,n^4 + 360\,n^3) q^3 + (-50\,n^5 + 630\,n^4 - 2160\,n^3 + 2160\,n^2) q^2 \\ + (24\,n^5 - 600\,n^4 + 3780\,n^3 - 8640\,n^2 + 6480\,n) q \\ + 144\,n^5 - 1656\,n^4 + 5760\,n^3 - 5400\,n^2 - 5184\,n + 7776].\end{aligned}$$

https://doi.org/10.1017/S0956792504005753 Published online by Cambridge University Press

Motivated by (6.36)–(6.38) we seek a local similarity solution of the form

$$h \sim (t_c - t)^{\alpha} F\left(\frac{(a-x)}{(t_c-t)^{\beta}}\right) \quad \text{as} \quad t \to t_c \quad \text{with} \quad (a-x) = O\,(t_c - t)^{\beta} \tag{6.39}$$

with $6\beta - n\alpha = 1$. If we include the correction term from (6.38) in the local behaviour of this similarity solution (as we outline below, this will in fact be the case only for sufficiently small q) then we are required to choose

$$\alpha = -\frac{qn - 6(\gamma n - 1)}{qn^2} \quad \beta = \frac{1-\gamma n}{qn}. \tag{6.40}$$

Thus we have

$$-\alpha F + \beta\eta \frac{dF}{d\eta} = \frac{d}{d\eta}\left(F^n \frac{d^5F}{d\eta^5}\right), \tag{6.41}$$

$$\text{as} \quad \eta \to 0^+ \quad F \sim \left(\frac{n^5}{72(n-2)(n-3)(n+6)(n-6)(2n-3)}\right)^{\frac{1}{n}} \eta^{\frac{6}{n}};$$

before addressing the behaviour as $\eta \to +\infty$, we count boundary conditions at $\eta = 0^+$, which involves setting

$$F = \left(\frac{n^5}{72(n+6)(2n-3)(n-2)(n-3)(n-6)}\right)^{1/n} \eta^{6/n} + \hat{F}$$

and linearising in $\hat{F}$ to give an Euler equation whose solutions take the form

$$\eta^{\frac{6}{n}+Q}$$

where the possible Q satisfy the sixth-order polynomial

$$\begin{aligned}
&n^5Q^6 + (-9\,n^5 + 36\,n^4)Q^5 + (540\,n^3 + 25\,n^5 - 270\,n^4)Q^4 \\
&+(-15\,n^5 + 600\,n^4 - 3240\,n^3 + 4320\,n^2)Q^3 \\
&\quad +(-26\,n^5 - 270\,n^4 - 19440\,n^2 + 5400\,n^3 + 19440\,n)Q^2 \\
&\quad +(-24\,\alpha\,n^6 + (156\,\alpha + 144)n^5 + (540\,\alpha - 1956)n^4 + \\
&\qquad (-5400\,\alpha + 6480)n^3 + (11664\,\alpha + 3240)n^2 - (7776\,\alpha + 38880)n + 38880)Q \\
&\qquad +144\,n^5 - 936\,n^4 - 3240\,n^3 + 32400\,n^2 - 69984\,n + 46656 = 0.
\end{aligned}$$

In Figure 15 we plot the corresponding roots for $n = 6.1$, $n = 7$ and $n = 10$, along with a close up view when $n \approx 6.27$. Since an admissible mode has $\mathrm{Re}(Q) > 0$, we observe that four roots are possible (either four real, two real and two complex, or four complex) over much of the range of α shown.

We start our discussion with the case of relatively small n, such that $\alpha = -1/(n+6)$ is larger than the repeated root of α, which we denote by $\alpha_c(n)$, at which the real roots with smallest $Q > 0$ become complex (the significance of this condition will become clearer later); we denote this range by $6 < n < n_c$ and find that $n_c \approx 6.27$ (see Figure 15). First we suppose that q is sufficiently small that it lies on the lowest branch with $Q > 0$ in

https://doi.org/10.1017/S0956792504005753 Published online by Cambridge University Press

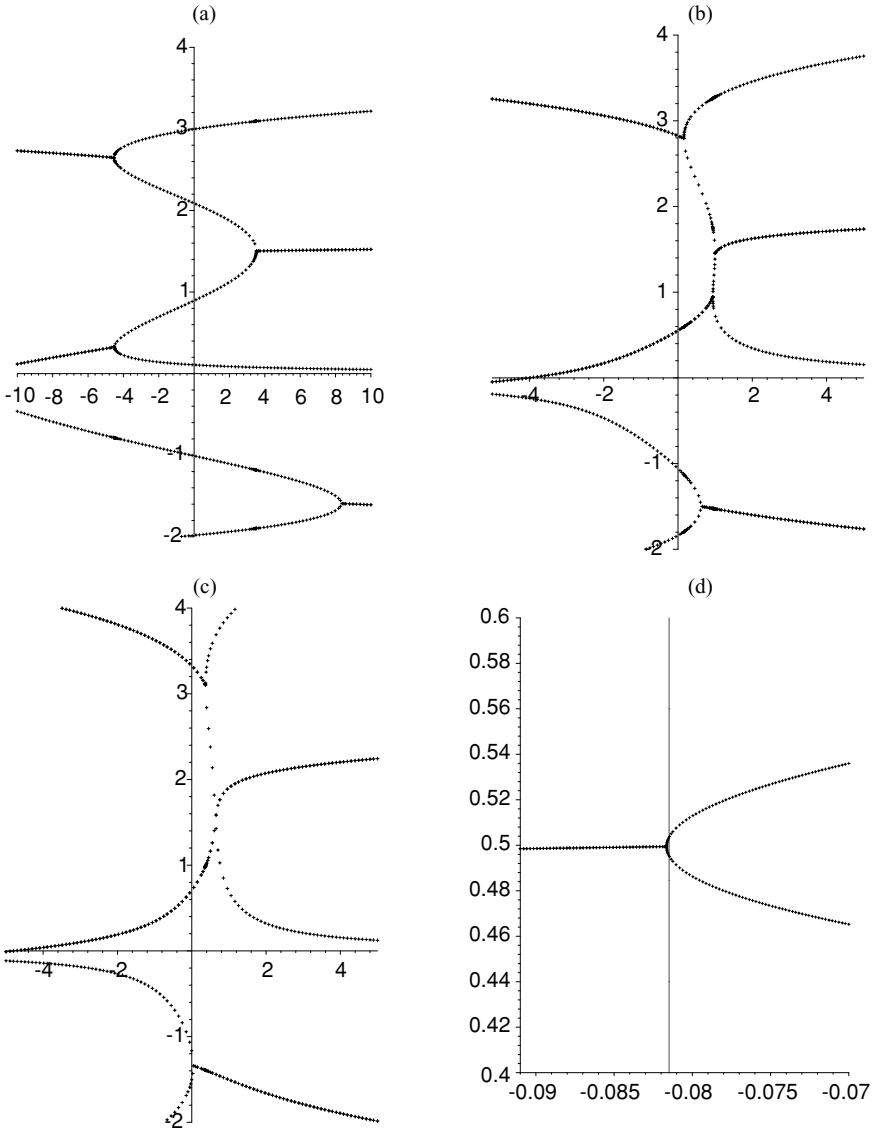


FIGURE 15. Plots of Re(Q) (vertical axis) against α (horizontal axis) for (a) $n = 6.1$, (b) $n = 7.0$, (c) $n = 10$, and (d) $n \approx 6.27$ where the turnover in the lower solution branch intersects with the line $\alpha = -1/(n+6)$ (also shown). The single curves arising from the merger of two others corresponds to two real roots becoming complex conjugates.

$\alpha > -1/(n+6)$. Prescribing the local behaviour in the form (6.38) (we shall address later whether or not such a condition is in fact applicable), where t_c is known in terms of Λ from the initial data, it is clear from Figure 15 that we are then left, as required, with three degrees of freedom as $\eta = 0$ (namely the upper three branches, of which the lower two are complex for sufficiently large α). Two possibilities then suggest themselves as

https://doi.org/10.1017/S0956792504005753 Published online by Cambridge University Press

$\eta \to +\infty$, namely

$$\text{as} \quad \eta \to +\infty \quad F \sim C\eta^{\alpha/\beta}, \tag{6.42}$$

where the (positive) constant C and the coefficients of two exponentially decaying terms give the required three degrees of freedom (α and β are known from the initial data via (6.41)) and

$$\text{as} \quad \eta \to +\infty \quad F \sim \kappa\eta, \tag{6.43}$$

where the (positive) constant κ and the coefficients of terms in η^0 and η^{5-n} provide the three degrees of freedom. In the case (6.42) it follows that

$$h(x, t_c) \sim C(a-x)^{\alpha/\beta} \quad \text{as} \quad x \to a^-, \tag{6.44}$$

with $\alpha > -1/(n+6)$, $\beta > 1/(n+6)$ being required for $\alpha/\beta > -1$ (finite mass) and with $\alpha/\beta < 6/n$ then necessarily applying. However, when (6.43) applies, additional regions are required, the asymptotic structure being as described in the previous subsection. In this case (6.27) is replaced by

$$\Lambda(t) = \kappa(t_c - t)^{\alpha-\beta},$$

so

$$\dot{b} \sim \frac{\beta-\alpha}{2}\left(\frac{\kappa}{10M}\right)^{\frac{1}{\beta-\alpha}}(a-b)^{-\frac{2}{\beta-\alpha}+1} \quad \text{as} \quad t \to t_c^-$$

and we recover (6.33) (which now describes the local behaviour of $h(x, t_c)$) with

$$\Lambda' = \Theta_\infty\left(\frac{\beta-\alpha}{2}\right)^{\frac{3}{3n-5}}(10M)^{-\frac{5}{3n-5}}\left(\frac{\kappa}{10M}\right)^{\frac{3}{(3n-5)(\beta-\alpha)}}, \quad p' = \frac{23-6/(\beta-\alpha)}{3n-5}. \tag{6.45}$$

Since

$$p' = \frac{23(n-6)\alpha - 13}{(1+(n-6)\alpha)(3n-5)} \tag{6.46}$$

we have

$$p' \to \left(\frac{23}{3n-5}\right)^- \quad \text{as} \quad \alpha \to +\infty,$$

so the current range complements that of Section 6.4.2, and

$$p' \to (-1)^+ \quad \text{as} \quad \alpha \to -1/(n+6),$$

coinciding with the exponent in (6.44) in this limit; moreover, in this latter limit the three relevant regions, $\eta = O(1)$, $a - x = O(1/\Lambda^{1/2})$ and $\zeta = O(1)$, each become of size $(t_c - t)^{1/(n+6)}$ and hence merge into one. The exponent p' in (6.46) satisfies

$$p' > \frac{6}{n} \quad \text{for} \quad \alpha > \frac{31-30n}{5(n+6)(n-6)} \tag{6.47}$$

in which case the solution can be continued through blow-up (in the sense that when $t = t_c$ a delta function is created at $x = a$, but the solution in $x < a$ can continue (with (6.33) providing the relevant local behaviour), and will subsequently experience infinite-time blow-up, as described in § 6.4; note from (6.46) that $p' < 1$). For smaller α we have $p' < 6/n$ and the solution cannot be continued past $t = t_c$ (the same conclusion applies

https://doi.org/10.1017/S0956792504005753 Published online by Cambridge University Press

to (6.44) for all relevant α; for $p < 6/n$ we conjecture that instantaneous blow-up occurs and we shall not discuss this regime further).

Having just outlined the behaviour we expect similarity solutions satisfying either (6.42) or (6.43) to exhibit, we now need to address the circumstances under which we expect such local solutions to be realised. Information in this regard can be deduced from asymptotic results (of which we omit almost all the details) in the following limits.

(1) $\beta \to \infty$, $n = O(1)$. The solution satisfying (6.42) can be constructed analytically in this limit and has $\Omega < 0$.

(2) $n \to 6^+$, $\beta = O(1)$. The solution which satisfies (6.43) can be constructed analytically and has $\Omega > 0$.

(3) $\beta \to \infty$, $n - 6 = O(1/\beta)$. Leading-order solutions can be constructed analytically, with (6.42) having $\Omega < 0$ and (6.43) having $\Omega > 0$.

(4) $\beta \to (1/(n+6))^+$, $6 < n < n_c$. Here we can exploit the exact first integral that exists for (6.41) when $\beta = -\alpha = 1/(n+6)$ to show that Ω has the same sign (which we expect to be positive) for both solutions (i.e. one satisfying (6.42) and the other (6.43)); indeed the former has a boundary layer solution given by the latter together with two further regions, essentially as in § 6.4.2.

Piecing together our conjectures from such information, we propose that for $n_c > n > 6$ both types of similarity solution exist for all $\beta > 1/(n+6)$ with that satisfying (6.43) having $\Omega > 0$ for all β but the one satisfying (6.42) having $\Omega < 0$ for $\beta > \beta^*(n)$ and $\Omega > 0$ for $\beta < \beta^*(n)$ for some $\beta^*(n)$ (the critical value $\beta^*(n)$ thus being a "second kind" similarity exponent whose evaluation would require very careful numerics); the appropriate similarity solution is thus determined for $\beta > \beta^*$ by the sign of Ω in the initial data (6.37). At $\beta = \beta^*$ it follows that $\Omega = 0$ holds when (6.42) pertains and the solution decays onto (6.36) more rapidly than the generic rate (i.e. the first correction term to (6.36) lies on the second branch in Figure 15 with positive Re(Q) rather than on the first). This leads us to suggest the following scenario which is closely analogous to "pushed" front (nonlinear) selection of travelling waves in reaction-diffusion problems (an analogy which can be made rather precise but at the cost of lengthier analysis than we would be justified in reporting here). For $\beta > \beta^*$ (where β is given by (6.40)), β is indeed determined by the value of q in the correction term in the initial data, with local behaviour at blow-up being of the form (6.44) if $\Omega < 0$ and (6.33), (6.46) if $\Omega > 0$. Conversely if (6.40) would imply $\beta < \beta^*$, then the required similarity solution has $\beta = \beta^*$, $\alpha = \alpha^* \equiv (6\beta^* - 1)/n$ and satisfies (6.42); since this similarity solution has larger β than those which would be naively selected (as above) via the initial data, the latter are unstable (being "overrun" by the (fast decaying) $\beta = \beta^*$ solution). We expect this second scenario (where $\alpha = \alpha^*$) also to apply generically for initial data having q lying on one of the higher branches in Figure 15, corresponding as it does to the maximal rate of decay as $\eta \to 0^+$ to (6.36) of any similarity solution satisfying a relevant boundary value problem.

Finally, we turn to the case $n > n_c$ which needs little further discussion. Two distinct scenarios are now in principle possible. For n sufficiently close to n_c we might expect the above scenario still to apply, with $\alpha^* > \alpha_c$. The second possibility would corresponding to "pulled" front (linear) selection in reaction-diffusion problems, and may perhaps apply for

https://doi.org/10.1017/S0956792504005753 Published online by Cambridge University Press

sufficiently large n, namely $n > n^* > n_c$, where n^* is defined by $\alpha^*(n^*) = \alpha_c(n^*)$ (assuming only one such switch in behaviour occurs); delicate numerical investigations would be required to pin down whether such as n^* exists. It would have each of the similarity solutions (i.e. (6.42) for $\Omega < 0$ and (6.43) for $\Omega > 0$) existing right down to the repeated root exponent $\alpha = \alpha_c > -1/(n+6)$ and providing the blow-up behaviour for the relevant (i.e. sufficiently small) q; for larger q, the exponent $\alpha = \alpha_c$ (having "critically damped" (maximal) rate of decay to (6.36)) will instead pertain in describing the blow-up behaviour, with two such solutions presumably being possible (one satisfying (6.42) and the other (6.43)).

To conclude this discussion we should note that other scenarios are far from out of the question, notably that the (6.43) solution (with $\Omega > 0$) remains stable down to $\alpha = -1/(n+6)$ for $n < n_c$ and down to $\alpha = \alpha^*$ for $n_c < n < n^*$ (if $n^* < \infty$ indeed exists). Investigation of such matters is hamstrung by the absence of a comparison principle and we shall not pursue them further. We have sought here to give an appropriate level of detail, illustrating the full range of blow-up behaviours that are possible without implementing an exhaustive analysis. We believe that the range $n > 6$ is a novel and noteworthy one, justifying the extent of the analysis we have given. For innocuous (finite mass) initial data, the solution can exhibit each of the following: instantaneous blow-up ($p < 6/n$); finite-time blow-up and film rupture ($p = 6/n$), having the possibility of continuing through blow-up having lost some of the mass to a delta function at $x = a$; infinite-time blow-up ($6/n < p < 1$), sometimes exhibiting as unusual type of pattern formation with large-time asymptotics comprising a sequence of spikes having different time dependencies (we use "humps" and "spikes" interchangeably here); infinite-time rupture (at $x = b \in [0, a)$) for $p = 1$ with Λ sufficiently large and with $b \to a$ for $6/n < p < 1$); and well-behaved evolution to a steady state ($p > 1$ and $p = 1$ with Λ sufficiently small). The possibility of finite-time film rupture for large n is particularly noteworthy, contrasting with the corresponding fourth-order case. The various types of blow up can be rather precisely characterised by the exponent p' in the solution which is "left behind" and by the exponents governing the time dependence of the (possibly multiple) spikes. What is especially striking about the case $n > 6$, in addition to this sensitivity just recorded to the local form of the initial data close to a zero in h (which is particularly pronounced when $p = 6/n$), is that this wide variety of behaviour is spontaneously generated, in the sense that it is not produced by additional source terms in the evolution equation (in contrast to the most familiar examples of blow-up and pattern formation); moreover, it is noteworthy that it is generated in an evolution equation which has two scaling invariants.

7 Discussion

We start by noting some clear quantitative differences from the fourth-order case. Firstly, in the latter case interface advance ($\dot{s} > 0$) is not possible for any non-negative mass-preserving solutions for sufficiently large n ($n \geqslant 3$), nor is drainage ($J < 0$ in the current notation) for $n \geqslant 2$. By contrast, while here there are windows ($5/2 \leqslant n < 5$ and $3/2 \leqslant n < 4$, respectively) in which the same constraints apply, now there are solution branches ($p = 5/n$ and $p = 5/(n+1)$, respectively; see Figure 1) on which expansion and

https://doi.org/10.1017/S0956792504005753 Published online by Cambridge University Press

drainage occur for large n; however, these branches correspond to solutions with very little regularity at the contact line (being highly underspecified) and it is not clear how such solutions could arise in practice. The most significant distinction is the entirely new parameter regime $n > 6$ which exhibits some unusual asymptotic behaviour and which, in particular, accentuates sharp decay in h for small h within the initial data into one or more "spikes" (i.e. mass gets dragged into the region of rapid variation in the initial data, a property for which one might envisage applications in image processing contexts). In this regard it is worth commenting briefly on the case $n > 6$ with a prewetting layer of small but non-zero thickness ϵ. For $6/n < p < 1$ the most noteworthy scalings take the form

$$t = \epsilon^{-\frac{np-6}{p}} T, \quad x = a + \epsilon^{\frac{1}{p}} X, \quad h = \epsilon g \tag{7.1}$$

whereby

$$\begin{aligned} &\frac{\partial g_0}{\partial T} = \frac{\partial}{\partial X}\left(g_0^n \frac{\partial^5 g_0}{\partial X^5}\right), \\ &\text{as} \quad X \to +\infty \quad g_0 \to 1, \\ &\text{as} \quad X \to -\infty \quad g_0 \sim \Lambda(T)(-X), \end{aligned} \tag{7.2}$$

where $\Lambda(T)$ is determined as part of the solution. The small T asymptotics of (7.2) are given by (i.e. match with) the large-time results of § 6.4, so that $\Lambda(T) \propto T^{(1-p)/(np-6)}$ as $T \to 0$ (cf. (6.27)). However, as $T \to \infty$ we have $g_0 \sim G(X/T^{1/6})$, so that $\Lambda(T) \propto T^{-1/6}$ and the spike near $x = a$ thus spreads back out and diminishes in height; this rearrangement influences the whole droplet for $t = O(\epsilon^{-(n-6)})$, before quasi-steady spreading finally occurs on the timescale $t = O(\epsilon^{-(n-5/2)})$, as described in § 3.3. For $p < 6/n$, the timescale (7.1) now describes the initial behaviour (consistent with instantaneous blow-up in the $\epsilon = 0$ limit problem); the asymptotics of the $T \to \infty$ limit then seem rather formidable, with a far from trivial structure of spikes arising (some insight into this can be gleaned via the limit $n \to 6$ with $|p - 1| = O(|n - 6|)$ which is more tractable that the more general case, but still not straightforward; as indicated below, the limit $n \to 6^-$ may be of relevance to very shear-thickening fluids). Nevertheless, it seems likely that true blow-up is avoided in the prewetted case (though spike heights tend to infinity as $\epsilon \to 0$), with the droplet ultimately spreading, again as described in § 3.3, and with spike structures of significant complexity arising over the intermediate time scales; such comments are necessarily somewhat speculative at this stage and the problem seems worthy of much more refined numerical experimentation. Given that (in the $\epsilon = 0$ case) finite-time blow-up in the separable solution occurs for $p = 6/n$, our conjecture of instantaneous blow up for $p < 6/n$ seems highly plausible but, in the absence of comparison principle, other possibilities (notably self-similar behaviour of the limit cycle form $\eta^{6/n}\phi(-\ln \eta)$ as $\eta \to 0^+$, where ϕ is periodic) cannot be ruled out on the basis of the analysis above.

Our next remarks relate to the physical realisability of the results. For power-law fluids in which the viscosity is proportional to the shear stress raised to the power $q - 1$ (so that Newtonian fluids have $q = 1$, shear-thinning ones $0 < q < 1$ and shear-thickening ones $q > 1$) it is implicit in King [16] that (1.1) with $n = (2q + 1)/q$ arises in a (very particular) parameter regime involving flow across a slightly-inclined planar substrate;

https://doi.org/10.1017/S0956792504005753 Published online by Cambridge University Press

the regime $2 < n < 3$ is then in principle realisable for shear-thickening fluids and $n > 3$ for shear-thinning ones. A rather less artificial limit involves power-law fluids spreading on a horizontal substrate, in which case, [16],

$$\frac{\partial h}{\partial t} = \frac{\partial}{\partial x}\left(h^n \left|\frac{\partial^5 h}{\partial x^5}\right|^{m-1} \frac{\partial^5 h}{\partial x^5}\right) \tag{7.3}$$

arises with $m = 1/q$, $n = m + 2$. The various critical exponents generalise to (7.3) as follows: $n = 2m/3$ (for 2/3), $3m/2$ (for 3/2), $(2m + 3)/3$ (for 5/3), $(3m + 2)/2$ (for 5/2), $3(m + 1)/2$ (for 3) and $4m + 2$ (for 6); it is worth stressing that, because these exponents arise from the behaviour local to the interface, the same critical exponents apply in higher dimensions (in addition, the self-similar results for the large-time behaviour, and so on, can be readily generalised to multi-dimensional problems). It follows in particular that sufficiently shear-thinning fluids, $q < 1/4$, lie in the regime $n < 3m/2$ and can therefore exhibit drainage and that very shear-thickening ones ($q \to 0$) have $n/(4m + 2) \to 1^-$, to which the limit $n \to 6^-$ of (1.1) mentioned above, in which spiking behaviour can occur on sufficiently short timescales, is pertinent.

Having shown that the sixth-order equation exhibits phenomena not present at all in the fourth-order case, it is mathematically a natural question whether this is the end of the story or whether the eighth-order case

$$\frac{\partial h}{\partial t} = -\frac{\partial}{\partial x}\left(h^n \frac{\partial^7 h}{\partial x^7}\right), \tag{7.4}$$

exhibits yet more new effects. The answer seem to be mixed, the key solution being the separable one

$$h = \left(\frac{n^7 (a - x)^8}{128(n + 6)(3n - 4)(5n - 8)(n - 2)(3n - 8)(n - 4)(n - 8)t}\right)^{1/n}. \tag{7.5}$$

The regime analogous to that with $n > 6$ above is now the finite one $4 < n < 8$ and this can again be expected to exhibit instantaneous blow-up and so forth (with sensitivity to the local form of the initial data). However, for $n > 8$, it seems likely that one reverts to a regime in which finite-time blow-up cannot occur (more specifically, for $1 < p < 2$ we expect behaviour analogous to that above for $n > 6$ with $6/n < p < 1$, but for $8/n < p < 1$ there can be expected to be a large-time local similarity solution with behaviour of the form (7.5) at infinity and for $p < 8/n$ the solution (7.5) is likely to apply locally at $x = a$ for all $t > 0$). More generally, the effect of increasing the order by two is that additional regimes of exponents n come in for large n, with the various critical exponents shifting their values of n; no further dramatic changes in behaviour with increasing order seem likely, however.

We have attempted here to make the first steps in advancing the formal understanding of (1.1) to a level comparable to that which is now in place for the corresponding fourth-order problem, seeking to provide fairly comprehensive insight by outlining in a concise fashion the behaviour of a variety of initial boundary value problems. It is worth remarking that the key critical exponent in the fourth-order case, namely $n = 3$, coincides

https://doi.org/10.1017/S0956792504005753 Published online by Cambridge University Press

with the most important physical application (namely to the spreading of thin films of Newtonian fluid) and this property has significant practical applications for moving contact lines. The current analysis shows that this is in some sense a coincidence, the corresponding exponent for the sixth-order case (namely $n = 5/2$) not corresponding to a Newtonian fluid. In closing, we note that we believe we have identified a considerable number of features of the behaviour of (1.1) which warrant investigation by rigorous means, especially as the problem is delicate numerically and formal asymptotics cannot, of course, provide definitive conclusions either. In such rigorous approaches an important role can be expected to be played (cf. Bernis & Friedman [3]) by the energy and "entropy" inequalities, obtained by integrating

$$\frac{\partial}{\partial t}\left(\frac{1}{2}\left(\frac{\partial^2 h}{\partial x^2}\right)^2\right) = \frac{\partial}{\partial x}\left(\frac{\partial^2 h}{\partial x^2}\frac{\partial^2}{\partial x^2}\left(h^n\frac{\partial^5 h}{\partial x^5}\right) - \frac{\partial^3 h}{\partial x^3}\frac{\partial}{\partial x}\left(h^n\frac{\partial^5 h}{\partial x^5}\right) + h^n\frac{\partial^4 h}{\partial x^4}\frac{\partial^5 h}{\partial x^5}\right) - h^n\left(\frac{\partial^5 h}{\partial x^5}\right)^2 \tag{7.6}$$

and

$$\frac{\partial}{\partial t}\left(\frac{h^{-(n-2)}}{(n-2)(n-1)}\right) = -\frac{\partial}{\partial x}\left(\frac{1}{n-1}h\frac{\partial^5 h}{\partial x^5} + \frac{\partial h}{\partial x}\frac{\partial^4 h}{\partial x^4} - \frac{\partial^2 h}{\partial x^2}\frac{\partial^3 h}{\partial x^3}\right) - \left(\frac{\partial^3 h}{\partial x^3}\right)^2, \tag{7.7}$$

respectively, with respect to x; in contrast to the fourth-order case there seem to be no straightforward generalisations of the latter involving other powers of h.

Acknowledgments

We gratefully acknowledge very helpful discussions with Mark Bowen and the financial support of the EPSRC.

Appendix: Numerical methods

We have used two methods to produce the numerical results; given some of the fine structure which arises, the application of more sophisticated numerical approaches would certainly be worthwhile. The majority of the simulations were based around the NAG routine D03PHF, which uses finite differences and the method of lines to solve general systems of parabolic-elliptic equations. To implement this method on the sixth-order equation we rewrite (1.1) as a system of three second order equations

$$\frac{\partial h}{\partial t} = \frac{\partial}{\partial x}\left(\left(h^2 + \hat{\epsilon}^2\right)^{\frac{n}{2}}\frac{\partial p}{\partial x}\right), \quad p = -\frac{\partial^2 m}{\partial x^2}, \quad m = -\frac{\partial^2 h}{\partial x^2}$$

where p is the pressure and m is the bending moment. Note that we have also replaced h^n with $(h^2 + \hat{\epsilon}^2)^{n/2}$ where $0 < \hat{\epsilon} \ll 1$; this avoids difficulties if h attempts to become negative. The boundary conditions are implemented by specifying either the associated flux ($h^n\partial p/\partial x$, $-\partial m/\partial x$ and $-\partial h/\partial x$, respectively) or by setting the particular variable to zero (e.g. $h(a, t) = 0$).

https://doi.org/10.1017/S0956792504005753 Published online by Cambridge University Press

The second method we employed was used to solve equation (1.1) for $n > 6$ with linear behaviour at the boundary. Though the NAG routine was able to solve this problem it was prohibitively slow and consequently we are grateful to Mark Bowen for writing an alternative code (the results of the two methods were indistinguishable when both could be applied). This approach splits equation (1.1) in the form

$$\frac{\partial h}{\partial t} = \frac{\partial J}{\partial x}, \quad J = h^n \frac{\partial^5 h}{\partial x^5},$$

then uses the implicit method

$$\frac{h_i^{k+1} - h_i^k}{\Delta t} = \frac{J_i^{k+1} - J_{i-1}^{k+1}}{\Delta x},$$

where the discretisation

$$J_i^{k+1} = \left(\frac{1}{2}\left(h_{i+1}^{k+1} + h_i^{k+1}\right)\right)^n \left(\frac{h_{i+3}^{k+1} - 5h_{i+2}^{k+1} + 10h_{i+1}^{k+1} - 10h_i^{k+1} + 5h_{i-1}^{k+1} - h_{i-2}^{k+1}}{\Delta x^5}\right)$$

is adopted. In this way we can construct an interlaced banded matrix with alternating entries of the unknowns h_i^{k+1} and J_i^{k+1}, i.e. $h_1,\ J_1,\ h_2, \ldots . J_{N-1},\ h_N$. At the boundaries of the domain the above discretisation uses the external ghost points h_{-1}, h_0, h_N and h_{N+1}. Finite differencing the boundary conditions, we can relate these unknown values to known values inside the numerical domain. The resulting system of nonlinear equations is then solved using Newton iteration with an adaptive time step, the time step being controlled by requiring the Newton iteration to converge within a certain number of iterations.

References

[1] Aronson,, D. G. (1986) The porous medium equation. In: *Some Problems in Nonlinear diffusion*, Fasano, A. and Primicerio, M. (eds.), *Lecture Notes in Maths 1224*, Springer-Verlag.

[2] Barrett, J. W., Langdon, S. & Nuernberg, R. (2004) Finite element approximation of a sixth order nonlinear degenerate parabolic equation. *Numer. Math.* **96**, 401–434.

[3] Bernis, F. & Friedman, A. (1990) Higher order nonlinear degenerate parabolic equations. *J. Diff. Eq.* **83**, 179–206.

[4] Bernis, F., Hulshof, J. & King, J. R. (2000) Dipole and similarity solutions of the thin film equation in the half line. *Nonlinearity*, **13**, 413–439.

[5] Bertozzi, A. L., Brenner, M. P., Dupont, T. F. & Kadanoff, L. P. (1994) Singularities and Similarities in Interface Flows. In: *Trends and Perspectives in Applied Mathematics*, Sirovich, L. (ed.). Springer-Verlag.

[6] Bowen, M. & King, J. R. (2001) Asymptotic behaviour of the thin film equation in bounded domains. *Euro. J. Appl. Math.* **12**, 135–157.

[7] Bowen, M., Hulshof, J. & King, J. R. (2001) Anomalous exponents and dipole solutions for the thin film equation. *SIAM J. Appl. Math.* **62**, 149–179.

[8] Constantin, P., Dupont, T. F., Goldstein, R. E., Kadanoff, L. P., Shelley, M. J. & Zhou, S.-M. (1993) Droplet breakup in a model of the Hele-Shaw cell. *Phys. Rev. E*, **47**, 4169–4181.

[9] Dupont, T. F., Goldstein, R. E., Kadanoff, L. P. & Zhou, S.-M. (1993) Finite-time singularity formation in Hele-Shaw systems. *Phys. Rev. E*, **47**, 4182–4196.

[10] Evans, J. D., Vynnycky, M. & Ferro, S. P. (2000) Oxidation-induced stresses in the isolation oxidation of silicon. *J. Eng. Math.* **38**, 191–218.

https://doi.org/10.1017/S0956792504005753 Published online by Cambridge University Press

[11] Hobart, K. D., Kub, F. J., Fatemi, M., Twigg, M. E., Thompson, P. E., Kuan, T. S. & Inoki, C. K. (2000) Compliant substrates: A comparative study of the relaxation mechanisms of strained films bonded to high and low viscosity oxides. *J. Electron. Mat.* **29**, 897–900.
[12] Hulshof, J. (2001) Some aspects of the thin film equation. *Proc. Euro. Cong. Math. Vol. II. Prog. in Math.* **202**, 291–301. Birkhauser-Verlag.
[13] Huang, Z. & Suo, Z. (2002) Wrinkling of a compressed elastic film on a viscous layer. *J Appl. Phys.* **91**, 1135–1142.
[14] King, J. R. (1986) Mathematical aspects of semiconductor process modelling. PhD thesis, University of Oxford.
[15] King, J. R. (1989) The isolation oxidation of silicon – the reaction-controlled case. *SIAM J. Appl. Math.* **49**, 1064–1080.
[16] King, J. R. (2001) Two generalisations of the thin film equation. *Math. Comp. Mod.* **34**, 737–756.
[17] King, J. R. & Bowen, M. (2001) Moving boundary problems and non-uniqueness for the thin film equation. *Euro. J. Appl. Math.* **12**, 321–356.
[18] Koch, M., Harris, N., Maas, R., Evans, A. G. R., White, N. M. & Brunnschweiler, A. (1997) A novel micropump design with thick-film piezoelectric actuation *Meas. Sci. Technol.* **8**, 49–57.
[19] Landau, L. D. & Lifshitz, E. M. (1986) *Theory of Elasticity*, 3rd Ed. Pergamon Press.
[20] Smith, W. R., Howison, S. D. & Mayers, D. F. (1996) Numerical and asymptotic solution of a sixth-order nonlinear diffusion equation and related coupled systems. *IMA J. Appl. Math.* **57**, 79–98.
[21] Smyth, N. F. & Hill, J. M. (1988) High-order nonlinear diffusion. *IMA J. Appl. Math.* **40**, 73–86.

https://doi.org/10.1017/S0956792504005753 Published online by Cambridge University Press